Dual-located WHIRLY1 affects salicylic acid homeostasis *via* coordination of ICS1, PAL1 and BSMT1 during *Arabidopsis* plant aging

Wenfang Lin[1], Hong Zhang[1], Dongmei Huang[1], Dirk Schenke [3], Daguang Cai [3], Binghua Wu*[2], Ying Miao*[1]

1 Fujian Provincial Key Laboratory of Plant Functional Biology, College of Life Sciences, Fujian Agriculture and Forestry University, 350002 Fuzhou, China；2 College of Horticulture Science, Fujian Agriculture and Forestry University, 350002 Fuzhou, China；3 Department of Molecular Phytopathology, Christian-Albrechts University of Kiel, Germany

*Corresponding author

Fujian Provincial Key Laboratory of Plant Functional Biology, Fujian Agriculture and Forestry University, Fuzhou 350002, China; Email: ymiao@fafu.edu.cn, binghua.wu@fafu.edu.cn, Phone: 0086 59186392987

Running head: WHY1 regulated SA homeostasis via ICS1，PAL1 and BSMT1

Article Length: main body of the text: 6843 words including Abstract 250, Introduction 838, Results 2599, Discussion 1522, Material and Methods 1503, Acknowledgements 131; 8 figures

The author responsible for distribution of materials integral to the findings presented in this article in accordance with the policy described in the Instructions for Authors is: Ying Miao (ymiao@fafu.edu.cn), Binghua Wu (binghua.wu@fafu.edu.cn). Y.M. designed the study. W.F.L. performed SA measurements, western blots, phenotyping, and qRT-PCR. D.H. performed, ChIP-seq, ChIP-qPCR, H.Z. performed plasmid constructs and promoter activation activity and the mutants screening. B.H.W performed microarray data analyses. W.F.L. and Y.M. analyzed the

data. Y.M. and D.S. wrote the paper. No conflict of interest.

Dual-located WHIRLY1 affects salicylic acid homeostasis *via* coordination of ICS1, PAL1 and BSMT1 during *Arabidopsis* plant aging

Abstract

Salicylic acid (SA) homeostasis determines also developmental senescence and is spatiotemporally controlled by various mechanisms, including biosynthesis, transport and conjugate formation. The alteration of WHIRLY1 (WHY1), a repressor of leaf natural senescence, with respect to allocation in the nucleus or chloroplast causes a perturbation in SA homeostasis, resulting in adverse plant senescence phenotypes. Loss of *WHY1* resulted in a 5 days earlier SA peak compared to wild type plants which accumulated SA at 42 days after germination. SA accumulation coincided with an early leaf senescence phenotype, which could be prevented by ectopic expression of the nuclear WHY1 isoform (nWHY1). However, expressing the plastid WHY1 isoform (pWHY1) greatly enhanced cellular SA levels. A global transcriptional analysis in WHY1 loss-of-function background by expressing either pWHY1 or nWHY1 indicated that hormone metabolism related genes were most significantly altered. The pWHY1 isoform predominantly affected stress related gene expression, while the nWHY1 controlled rather developmental gene expression. Chromatin immunoprecipitation-qPCR (ChIP-qPCR) assays indicated that nWHY1 directly binds to the promoter region of isochorismate synthase (*ICS1)* to activate *its* expression at later stage, but indirectly activated S-adenosyl-L-methionine-dependent methyltransferase (*BSMT1)* gene expression *via* ethylene response factor 109

(ERF109), while repressing phenylalanine ammonia lyase (*PAL1)* expression *via* R2R3-MYB member 15 (MYB15) at the early stage of development. Interestingly, rising SA levels exerted a feedback effect by inducing nWHY1 modification and pWHY1 accumulation. Thus, the alteration of WHY1 organelle isoforms and the feedback of SA intervened in a circularly integrated regulatory network during developmental or stress-induced senescence in *Arabidopsis*.

Keywords: dual-located WHIRLY1, SA homeostasis, plant senescence, feedback loop, *Arabidopsis thaliana*

Introduction

Salicylic acid is crucial for plant growth, responses to pathogens, e.g. by programmed cell death and environmental responses. Its homeostasis is temporally and spatially controlled by various mechanisms, including biosynthesis, transport and conjugate formation. For example, leaf development in *Arabidopsis* was regulated by SA biosynthetic / signaling genes. Early leaf senescence is a result of SA overproduction in mutants such as isochorismate synthase (ICS1) and phenylalanine ammonia lyase

(PAL) overexpression lines (Love et al., 2008; Rivas-San et al., 2011), whereas the hypersensitive response (a fast form of programmed cell death) have been intensively investigated in the S-adenosyl-L-methionine-dependent methyltransferase (*bsmt1)* mutant (Vlot et al., 2009). There are two main SA biosynthetic pathways in plants: the phenylalanine ammonia lyase (PAL) pathway and the isochorismate (IC) pathway, both depending on the primary metabolite chorismate (Dempsey et al. 2011). In the PAL pathway, the chorismate-derived L-phenylalanine is converted into SA *via* either benzoate intermediates or coumaric acid through a series of enzymatic reactions involving PAL, benzoic acid 2-hydroxylase (BA2H), and other uncharacterized enzymes (Leon et al. 1995b). Approximately 10% of defense-related SA is produced by the cytosolic PAL pathway and in Arabidopsis four PAL enzymes have been identified. In the IC pathway, chorismate is converted in a two-step process to SA *via* isochorismate involving isochorismate synthase (ICS) and isochorismate pyruvate lyase (IPL). In *Arabidopsis*, two ICS enzymes have been described to convert chorismate to isochorismate, but in recent studies another isochorismate synthase was identified (Rekhter et al. 2019; Torrens-Spence et al. 2019). This pathway accounts for ~90% of the SA production generated by the plastid-localized ICS1 inducible by pathogens and UV light (Wildermuth et al. 2001; Garcion et al. 2008). Endogenous SA undergoes a series of chemical modifications including hydroxylation, glycosylation, methylation and amino acid conjugation. These modifications directly affect the biochemical properties of the SA derivatives, and play a pivotal role in SA

88 catabolism and homeostasis to regulate leaf senescence (Zhang et al. 2013). It has
89 been shown that SA affects regulation of gene expression during leaf senescence
90 (Morris et al. 2003; Vogelmann et al.2013; Zhang et al. 2013; 2017) and in advancing
91 flowering time in *Arabidopsis thaliana* (Martínez et al. 2004), as well as in inhibiting
92 seed germination (Alonso-Ramirez et al. 2009; Lee et al. 2013). Although SA
93 biosynthesis and its function in both local and systemic acquired resistance (SAR)
94 against microbial pathogens and in plant development were well understood (Park et
95 al. 2007; An and Mou, 2011), the underlying molecular mechanism of free SA
96 homeostasis in cells is less clear.
97 WHIRLY family proteins are dually located in both the nucleus and organelles, and
98 perform numerous cellular functions in both locations (Krause et al. 2005; Grabowski
99 et al. 2008). In the nucleus, WHIRLY1 (WHY1) protein was found to regulate the
100 expression of genes related to defense and senescence by binding to their respective
101 promoters (Desveaux et al. 2000; Desveaux et al. 2004; Xiong et al. 2009; Miao et al.
102 2013; Krupinska et al. 2013). WHY1 protein binds for example to the promoter of
103 *WRKY53* and repress *WRKY53* and *WRKY33* expression in a
104 development-dependent manner during early senescence in *Arabidopsis* (Miao et al.
105 2013; Ren et al. 2017), while it activates the *HvS40* gene during natural and
106 stress-related senescence in barley (*Hordeum vulgare*) (Krupinska et al. 2013) and
107 *PsbA* gene expression in response to chilling treatment in tomato (Zhuang et al. 2018).
108 In the nucleus, WHY1 protein also modulates telomere length by binding to their

109 *AT*-rich region (Yoo et al. 2007) and affects microRNA synthesis (Swida-Barteczka et
110 al. 2018). Moreover, in chloroplasts, WHY1 has a function on organelle genome
111 stability, facilitating accurate DNA repair (Cappadocia et al. 2010, 2012; Lepage et al.
112 2013) and affects RNA editing/splicing (Prikryl et al., 2008; Melonek et al. 2010). The
113 intracellular localization of WHY1 and/or the developmental stage of the plants may
114 contribute to its various functions (Ren et al. 2017). Furthermore, WHY1 has been
115 reported to be involved in (a)biotic stress signaling pathways, e.g. in response to
116 chilling (Zhuang et al. 2018), high light (Kucharewicz et al. 2017), N deficiency
117 (Comadira et al. 2013), reactive oxygen species (Lin et al. 2019; Lepage et al. 2013),
118 hormones such as SA and abscisic acid (Xiong et al. 2009; Isemer et al. 2012) and
119 defense signaling, being e.g. required for SA- and pathogen-induced PR1 expression
120 (Desveaux et al. 2005).
121 In this study, we extend the roles of the dual-located WHY1 protein with respect to SA
122 biosynthesis *via* regulating *PAL1* and *ICS1* expression and SA modification *via*
123 affecting *BSMT1* gene expression, in a developmental dependent manner. Moreover,
124 the cellular SA level affected the distribution and status of WHY1 protein in the
125 nucleus and in plastids, suggesting a feedback mechanism to regulate SA
126 homeostasis. Further, globally analysis of gene expression in loss-of WHY1 and
127 gain-of pWHY1 or nWHY1 indicated that the levels of hormone metabolism related
128 genes were significantly altered. Our results provide the first evidence that the
129 dual-located WHY1 protein exerts a novel function in both nucleus and chloroplasts to

fine-tune SA homeostasis affecting plant aging in *Arabidopsis*.

Results

WHY1 changes the gene expression level of *PAL*, *ICS* and *BSMT1* and SA contents during plant aging

. To explore how WHY1 involves in the SA metabolism pathways (Figure 1a), we used the *why1-1* mutant previously deployed in several of our studies (Miao et al. 2013; Ren et al. 2017; Lin et al. 2019). This *why1-1* mutant displays an early senescence phenotype (Miao et al. 2013), similar to the S-adenosyl-L-methionine-dependent methyltransferase (*bsmt1*) mutant (Vlot et al. 2009) and the SA 3-hydroxylase (*s3h*) mutant (Zhang et al. 2013). We analyzed the expression levels of *ICS, PAL*, *BSMT1*, encoding a protein with both benzoic acid (BA) and SA carboxyl methyltransferase activities, and salicylic acid glucoside/glucose ester modification enzymes such as *UGT71B1, UGT89B1* or *UGT74F2* (Dempsey et al. 2011) in the *why1* mutant compared to WT during plant development from 28 to 42 days after germination (dag). Interestingly, loss-of-*WHY1* increased the transcript level of *PAL1* and *PAL2* at 37 dag, but greatly decreased the transcript level of *BSMT1* at 35 and 37 dag and of *ICS1* at 42 dag (Figure 1b), while the transcript levels of *UGT71B1, UGT74F2*, *UGT89B1* and *S3H* were not altered in the *why1* mutant during plant development (Supplementary Fig S1).

Thus, we tested whether SA contents also changed in the *why1* mutant during plant aging. The SA contents including conjugated and free type of SA of the *why1* and WT

plants were measured with a HPLC assay during the period from 28 dag to 58 dag of plant development. Our results indicate that *loss-of-WHY1* made both conjugated SA and free SA peak 5 days earlier (at 37 dag) than in wild type (Figure 1c-d).

In order to genetically confirm this hypothesis, we produced t*he why1pal1, why1sid2, why1pal1sid2, why1bsmt1* double/triple mutants (Supplementary Fig S2) and measured the SA contents in these mutants during plant aging (Figure 1e). Interestingly, the early SA peak disappeared in the *why1pal1* line at 37dag, showing a similar SA profile as the wild type, while SA accumulation in *why1* mutants combined with *bsmt1* mutation were not that strongly affected, displaying the same early senescent phenotype as the *why1* line. However, SA accumulation in *why1* combined with *sid2* (ics1) was inhibited at 42 dag. The *whylpal1sid2* triple mutant showed a delay senescence phenotype and had again no earlier SA peak even maintain low level of SA at 37 and 42 dag during plant development, suggesting that PAL activity is crucially important for SA accumulation at early stage. Thus, we genetically confirmed that SA homeostasis in cells is affected by WHY1 predominantly by its effect on PAL1.

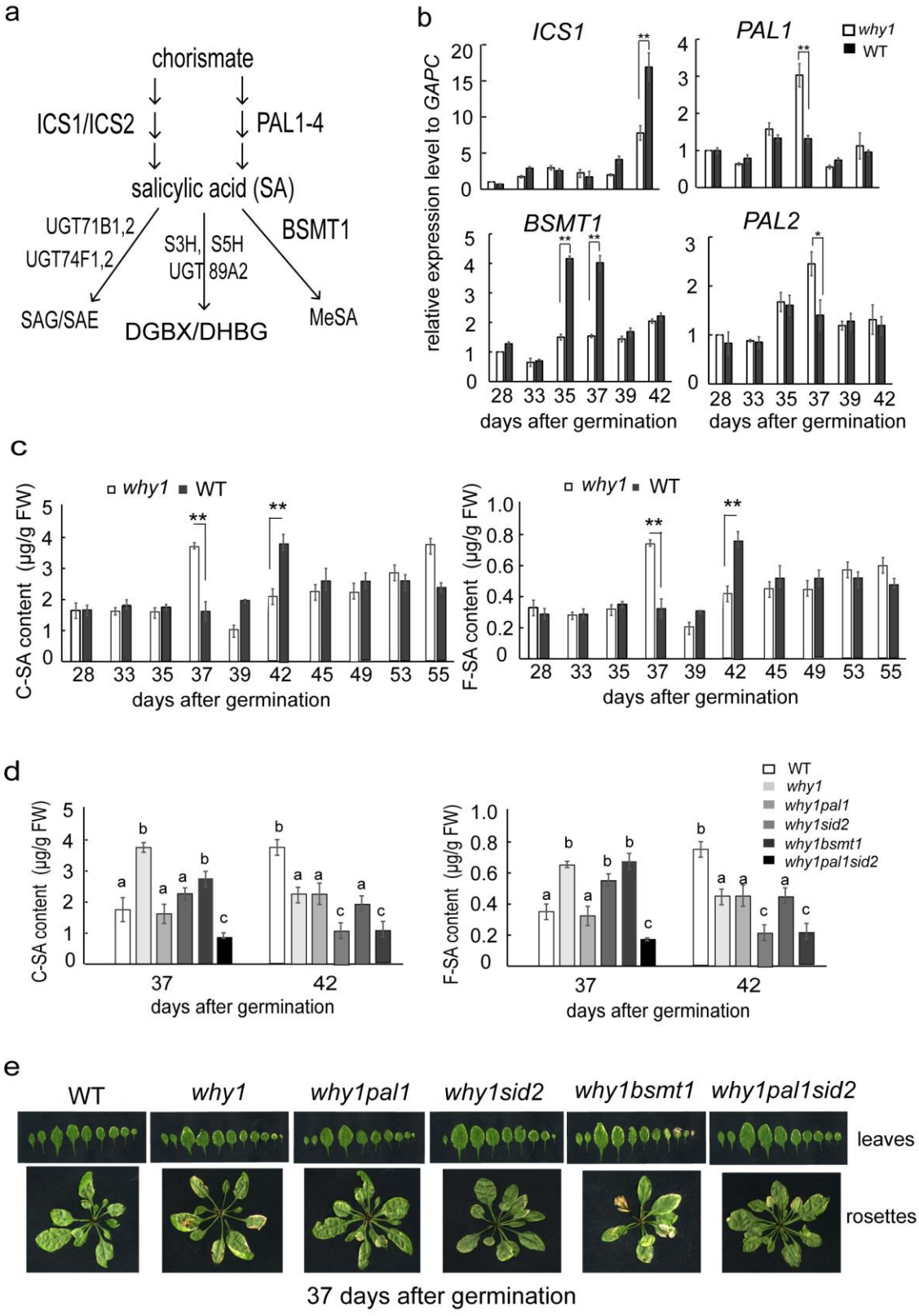

Figure 1. The variation transcript level of genes encoding key enzymes related to SA metabolism pathway and SA contents in the *why1* line during the development

a. SA metabolism pathway in the cell. b The variation transcript level of genes encoding key enzymes related to SA metabolism in the *why1* line during plant development. c. Content of conjugated (C-SA) and free (F-SA) salicylic acid in wild type and *why1* mutant during the period of 28 to 55 days after germination (dag); d. Changes of conjugated and free salicylic acid contents in a series of double mutants with focus on 37 and 42 dag. f. Senescence phenotype of 37 dag old double mutants. The relative expression level normalized to *GAPC*, wild type at 28 dag (b) was setup as 1. The standard error bars present three time biological replicates and three time techniques replicates, the values are shown as means ±SD. Asterisks (*P < 0.05, **P < 0.01) show significant differences to wild type line according to either two-way ANOVA or pair-wide multiple t-tests.

nWHY1/pWHY1 affects the gene expression level of *PAL1*, *ICS1* and *BMST1* as well as SA homeostasis during plant aging

As we knew, WHY1 is dual-located in the nucleus and plastids (Grabowski et al. 2008). To clarify which isoform of WHY1 affects SA metabolism and its homeostasis, we complemented the *why1* background line with pWHY1，nWHY1 and pnWHY1 under *35S* promoter control (Lin et al. 2019), and analyzed the transcript levels of *PAL*, *ICS, and BSMT1* from 28 dag to 42 dag. Complementation with nWHY1 or full length WHY1 (pnWHY1) restored wild type transcript levels of *PAL1, PAL2* and *BSMT1*, while the *nWHY1/why1* line had even lower *PAL1* expression level at 37 dag and 42

dag compared to WT. Surprisingly, complementation with pWHY1 not only pronounced the transcript level of *PAL1* two folds and repressed the transcript level of *BSMT1* at 37 dag, but also significantly increased the transcript level of *ICS1* at 42 dag, (Figure 2a). Measuring the SA contents in the complemented *why1* mutant background from 28 to 42 dag, both *nWHY1/why1* and *pnWHY1/why1* lines significantly restored wild type SA accumulation of the *why1* line until 37 dag and in the *nWHY1/why1* mutant the SA content was even lower at 42 dag. However, pWHY1 significantly pronounced SA accumulation during the whole period of development (Figure 2b), indicating that nWHY1 somehow repressed SA accumulation via suppression of *PAL1* expression. On the other hand, pWHY1 might pronounce SA accumulation via repressing *BSMT1* during the early stages and promoting *ICS1* at the late stage, in a developmentally dependent manner.

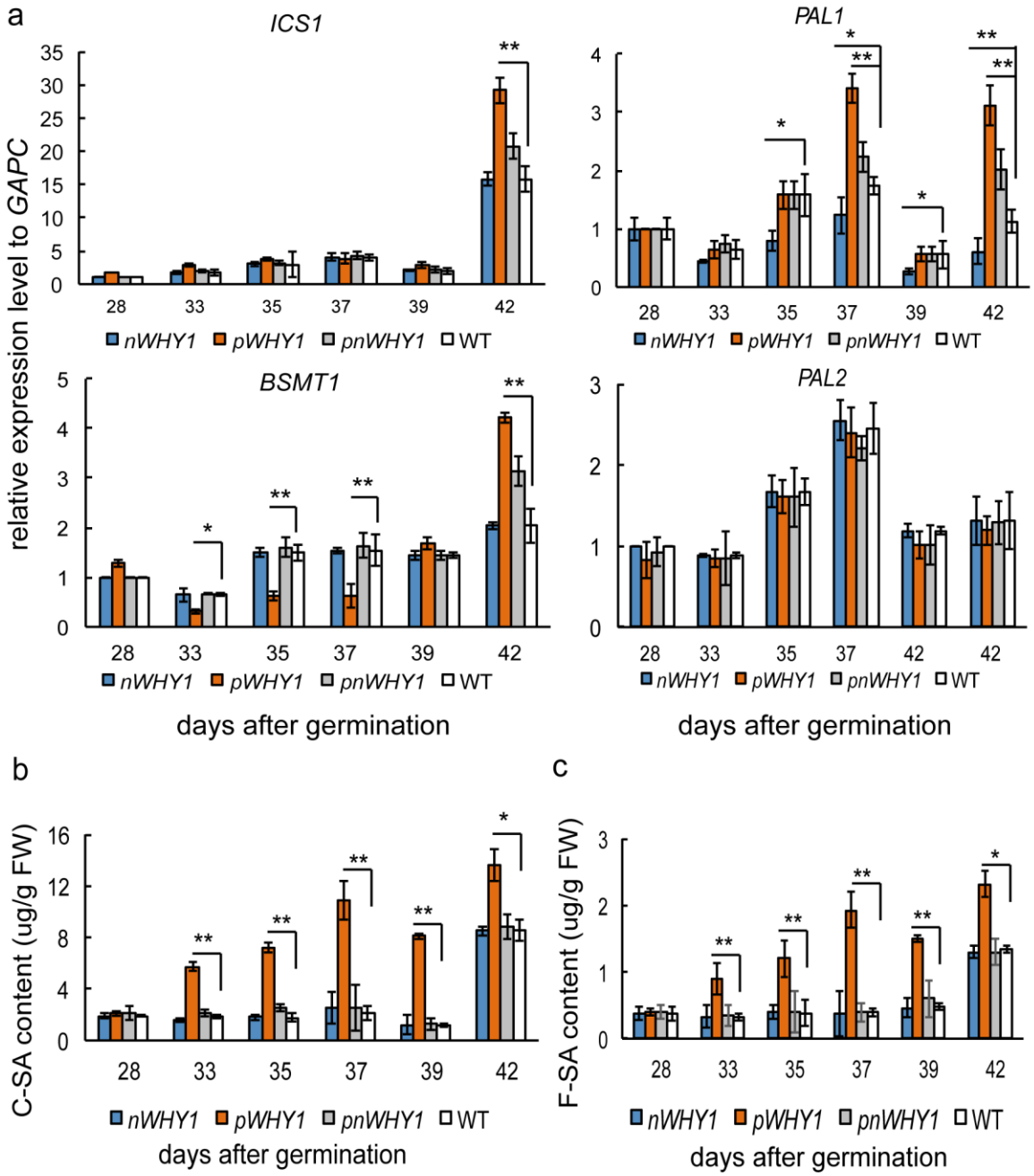

Figure 2. Transcript level analysis of genes encoding key enzymes related to SA metabolism pathway (a) and SA contents (b) in the *pWHY1/why1*, *nWHY1/why1*, and *pnWHY1/why1* transgenic plants compared to wild type from 28 to 42 dag during plant development.

The standard error bars present three time biological replicates, the values are shown as means±SE. Asterisks (*P < 0.05, **P < 0.01) show significant differences to WT

209 within the respective conditions according to Student's t test.

210

211 **Hormone- related gene enrichment in "compartmental WHY1" transgenic plants**

212 In order to globally understand the differences and similarities of the nuclear
213 transcriptome response between pWHY1 and nWHY1, a microarray sequencing
214 analysis was deployed. Phenotypic differences were observed in the short term
215 response and to avoid a long term secondary artifact caused by continuous
216 expression, an estradiol-inducible promoter was used to generate "inducible
217 compartmental WHY1" transgenic plants (*VEX:pWHY1/why1* and *VEX:nWHY1/why1*)
218 as described in Ren et al., (2017). We found that WHY1 protein level increased about
219 14 folds after two hours induction with 20 µM estradiol (Ren et al. 2017). The total
220 RNA isolated from the 5 week old rosette leaves of inducible *VEX:pWHY1/why1* and
221 *VEX:nWHY1/why1* plants before (0h) and after estradiol application (2h), as well as
222 from *why1* and WT plants was used for transcriptome analysis by ATH1 *Arabidopsis*
223 GeneChip microarrays with two biological replicates. Comparing the transcriptome of
224 inducible pWHY1 plants to that of non-inducible pWHY1 plants revealed a complex
225 genetic reprogramming with 1165 and 4560 transcripts being at least 2-fold up- and
226 down- regulated, respectively. Comparison of inducible nWHY1 plants to that of
227 non-inducible nWHY1 plants revealed also a complex genetic reprogramming with
228 920 and 3965 transcripts up- and down- regulated, respectively. Transcriptomic
229 comparison of the *why1* mutant to WT plants identified 4432 and 1190 transcripts up-

and down- regulated, respectively (Supplementary Fig S3).

To visualize gene expression reprogramming in the *VEX:pWHY1 VEX:nWHY1* and the *why1* plants, their entire nuclear transcriptome was subjected to MapMan analysis allowing the identification of biological processes with significant alterations (Thimm et al., 2004). The hormone metabolism pathways are significantly overrepresented after induction of pWHY1, nWHY1, or by loss-of WHY1, affecting especially auxin, jasmonic acid (JA) and ethylene metabolism, as well as SA metabolism (Figure 3, Supplemental dataset1-4). The regulation of secondary metabolism and stress are also significantly enriched after induction of pWHY1 expression (Figure 3a). These stresses are associated with biotic stresses and abiotic stresses responses that are related to redox imbalance. They mostly are up-regulated by pWHY1 (Figure 3a). In contrast the regulation of RNA, development and signaling terms are significantly enriched after induction of nWHY1 expression. Since the opposite regulation of signaling, development, RNA and transport terms is observed in loss-of WHY1 plants (Figure 3a), these changes can be attributed to the inducible expression of pWHY1 or nWHY1 (Figure 3a). Globally, a net enrichment of biological processes linked to hormone metabolism is found within the most significantly differential expressed genes after induction of pWHY1 or nWHY1 or deletion of WHY1 (Figure 3b); a net enrichment for biological processes linked to hormone metabolism, secondary metabolism and photosynthetic stress is found within the most differentially expressed genes in inducible pWHY1 line (Figure 3b), while a net enrichment for biological

processes linked to RNA regulation, development or signaling is found within the most differentially expressed genes in inducible nWHY1 line (Figure 3b) and a net enrichment for biological processes linked to photosynthesis and signaling or development or RNA regulation is found within the most differentially expressed genes in the *why1* line (Figure 3b).

a

VEX:pWHY1

Functional Group	Representation	P-value
Hormone metabolism	-	3.25E-6
Secondary metabolism	+	2.25E-4
Stress	+	5.32E-4
Miscelleanous	+	9.76E-3
Photosynthesis	-	2.13E-2

VEX:nWHY1

Functional Group	Representation	P-value
Hormone metabolism	-	6.25E-6
RNA regulation	-	3.25E-3
Development	-	2.32E-3
Miscelleanous	+	7.76E-3
Signaling	+	1.13E-2

why1

Functional Group	Representation	P-value
Hormone metabolism	+	2.49E-16
Photosynthesis	+	6.26E-14
RNA	+	4.35E-7
Signaling	-	2.81E-4
Development	+	4.26E-4
Miscelleanous	-	2.19E-3
Stress	-	3.89E-3
Transport	+	8.94E-3

b

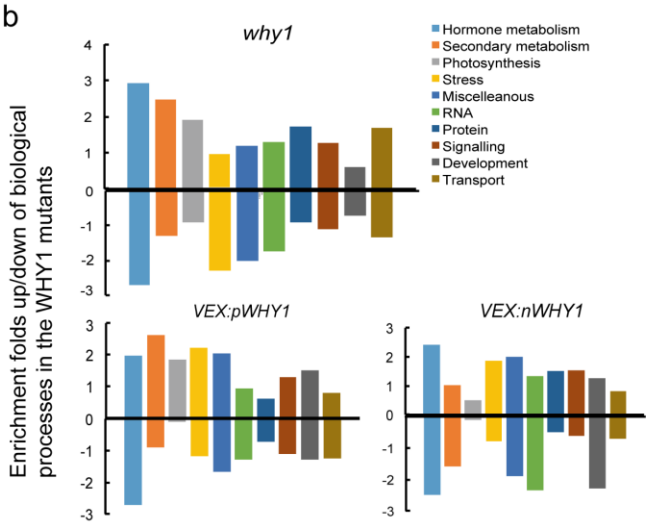

c

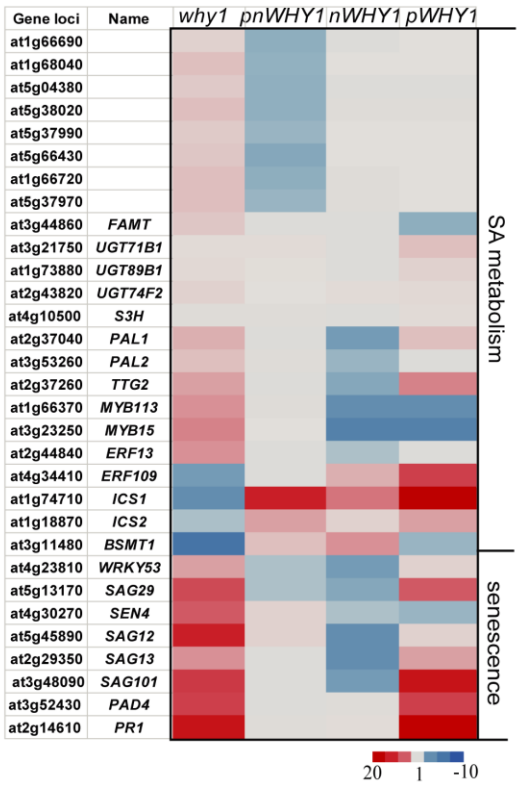

Figure 3. The V*EX:pWHY1*, *VEX:nWHY1* and the *why1* mutants exhibits a complex nuclear genetic reprogramming.

a. MapMan analysis for gene ontology terms enrichment of the entire *VEX:pWHY1*,

VEX:nWHY1 and the *why1* nuclear transcriptome.

b. Histogram presenting the ratio of differentially expressed genes enrichment changes of selected biological process of the *VEX:pWHY1, VEX:nWHY1* and the *why1* transcriptome.

c. The heatmap of SA metabolism related gene expression levels of the *pWHY1/why1*, *nWHY1/why1*, *pnWHY1/why1* plants, and the *why1* mutants. *VEX:pWHY1*, *VEX:pWHY1/why1; VEX:nWHY1, VEX:nWHY1/why1*

Among the differentially expression genes, 153 of differentially expression genes overlay between inducible pWHY1 and nWHY1 lines. Among them, 42 of hormone-related gene expressions were up- or down- expression in the pWHY1 or *why1* lines, including SA, JA, IAA and ethylene metabolism and signaling related genes (Figure 3, Supplementary dataset1-4). The 24 highest expressed or suppressed genes in the pWHY1, nWHY1 or the *why1* plants, which encode key components of the SA metabolism pathway including ICS1, ICS2, PAL1, PAL2, UGT71B1, UGT89B1, UGT74F2, BSMT1, as well as SA signaling related genes, or senescence / cell death related genes are shown in the heatmap (Figure 3c).

WHY1 directly binds at the promoter region of *ICS1* and indirectly affects *PAL1* and *BSMT1* expression in a developmental dependent manner

WHY1 was first reported as a transcription factor in the nucleus (Marechal et al. 2000). To investigate whether WHY1 directly regulates *ICS1, PAL1/PAL2, BSMT1* gene

expression, we analyzed our previous ChIP-seq dataset and above microarray dataset, and found that *ICS1, MYB15* and *ERF109* are direct targets of WHY1 (Miao et al. 2013; and Figure 4a), but *PAL1* and *BSMT1* are not. A search for transcription factor binding motifs in promoter regions of *ICS1, MYB15, ERF109, PAL1*, and *BSMT1* genes was conducted with PlantCARE (Lescot et al. 2002) and resulted in two w-boxes, six MYC elements, and four MYB motives in the promoter of *PAL1;* 6xERE elements in the *BSMT1* promoter (Figure 4b) as well as several GTNNNNAAT and AT-rich motives in the *ICS1, MYB15,* and *ERF109* promoters. In order to clarify the relationship among them, firstly, we confirmed WHY1 binding at the target genes by chromatin immunoprecipitation qPCR (ChIP-qPCR) using leaf material from 37 and 42 dag of expressing HA-tagged WHY1 under its native promoter (P_{why1}*:WHY1-HA)* as described in previous work (Miao et al. 2013). The putative cis elements found in *WRKY53, ICS1, MYB15*, *ERF109*, and *WRKY33* promoters, included several GTNNNNAAT or AT-rich motives (Figure 4b), and were enriched 5-20 fold (Figure 4c). The regions containing GTNNNNAAT and AT-rich motives of *MYB15, ERF109*, and *WRKY53* were enriched 10-15 folds at 37 dag, while fragments of *ICS1* and *WRKY33* could not be detected at 37 dag, but together with *MYB15* and *WRKY53* a high enrichment was observed at 42 dag (Figure 4c). Furthermore, the expression levels of these genes were analyzed by quantitative reverse transcription PCR (qRT-PCR) at 37 and 42 dag in *why1* and WT plants. WHY1 binding negatively correlated with gene expression in the knockout background of *ERF109* at 37 dag and

ICS1 at 42 dag and positively with *MYB15* expression at both 37 and 42 dag. While *WRKY53* expression is positively correlated in *why1* plants at 37 dag, *WRKY33* was up-regulated at 42 dag. Thus, WHY1 appears to exert either negative effects on gene expression (WRKY53, WRKY33 and MYB15) or causes activation of its target genes, such as *ERF109* and *ICS1* depending on the developmental stage.

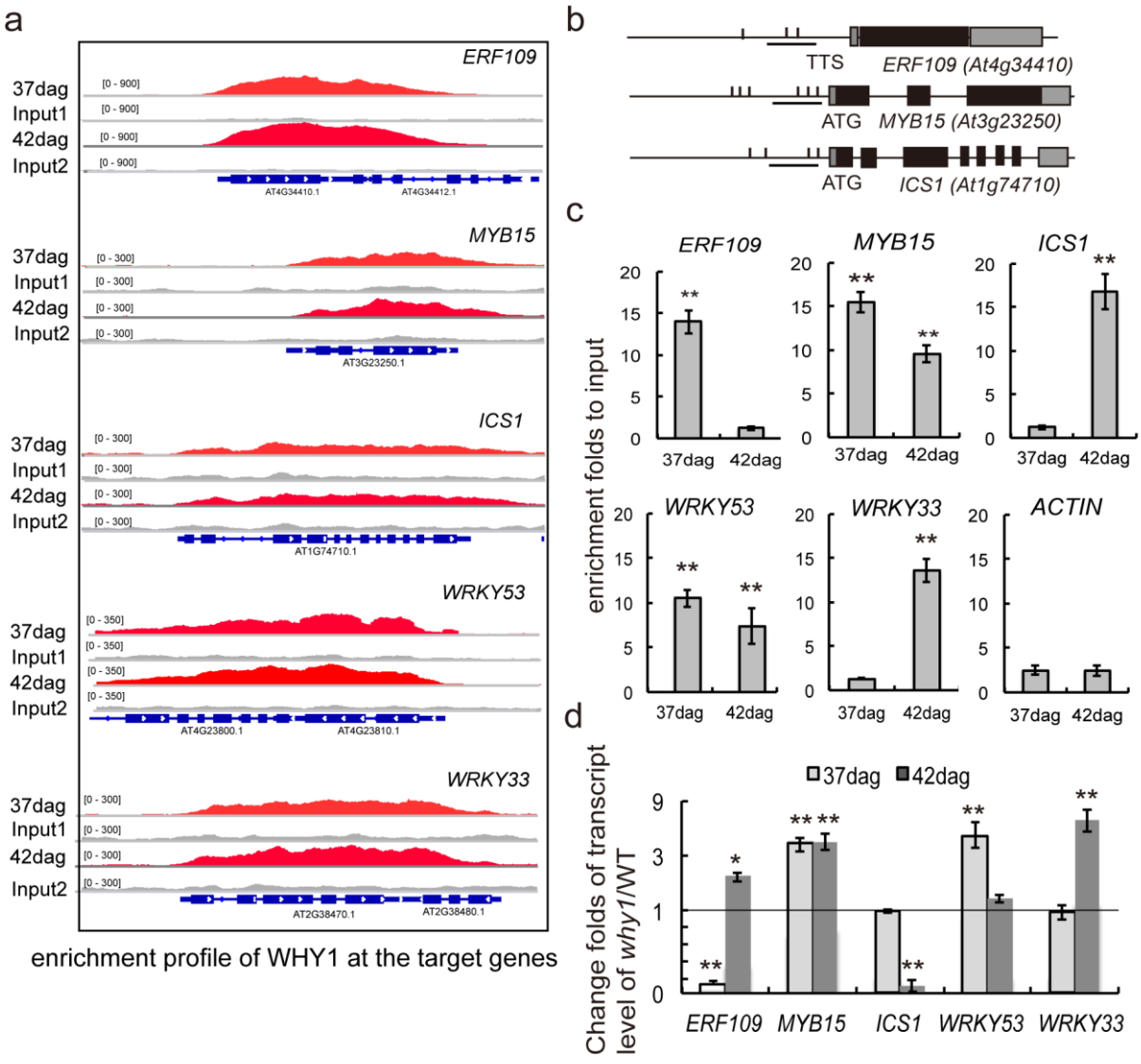

enrichment profile of WHY1 at the target genes

Figure 4. WHY1 activates/represses target gene expression

a. Enrichment profiles of WHY1 protein in five target genes: *ERF109, MYB15, WRKY33, ICS1*, and *WRKY53* by ChIP-seq; b.Position of promoter motives

(*GTNNNNAAT plus AT-rich*) of WHY1 target genes; c. Enrichment folds of WHY1 at the promoters of target genes by ChIP-qPCR at 37 and 42 days after germination; d. The expression levels of target genes at 37 and 42 days after germination in the *why1* mutant compared to WT. The error bars represented SD from three biological replicates. Asterisks indicated significant differences from the *ACTIN* according to two-tail Student's t test (* denotes $P < 0.05$, ** for $P < 0.01$).

In order to further verify the activation or repression activity of WHY1, the promoter sequences of *WRKY53, ICS1, MYB15, ERF109, PAL1* and *BSMT1* were cloned into dual-luciferase vectors and applied in a transient expression assay using *Nicotiana benthamiana* leaves (Hellens et al., 2005). In addition to measure promoter activation or repression by WHY1, also MYB15, and ERF109 were included in the analysis to investigate indirect effects of WHY1 in the nucleus. The coding sequences of WHY1, MYB15 and ERF109 were cloned under the control of the Arabidopsis *ACTIN1* promoter (*ACTIN:WHY1-HA, ACTIN:MYB15-HA,* and *ACTIN:ERF109-HA*) (Figure 5a), and co-infiltrated with the reporter vector to drive LUCIFERASE (LUC) expression (Hellens et al., 2005). We then measured the LUC and RENNILASE (REN) luminescence ratio (i.e. LUC/REN ratio) in infiltrated leaves. To assess any basal activation or repression of putative promoters, a mini-*GAL4* promoter vector was used in each co-infiltration experiment as a control; the *WRKY53* promoter was used as a positive control. The results showed that WHY1 activated promoters of *ICS1* and

331 *ERF109*, but it repressed the promoters of *MYB15* and *WRKY53* displaying the
332 opposite expression pattern of the why1 knockout plants (Figure 4b). The transcription
333 factors MYB15 and ERF109 were able to activate *PAL1, PAL2* and *BSMT1* gene
334 expression, respectively (Figure 5b-c). Therefore, WHY1 directly activated *ICS1*
335 expression and indirectly affected *PAL1, PAL2* and *BSMT1* gene expression *via*
336 MYB15 and ERF109, respectively.

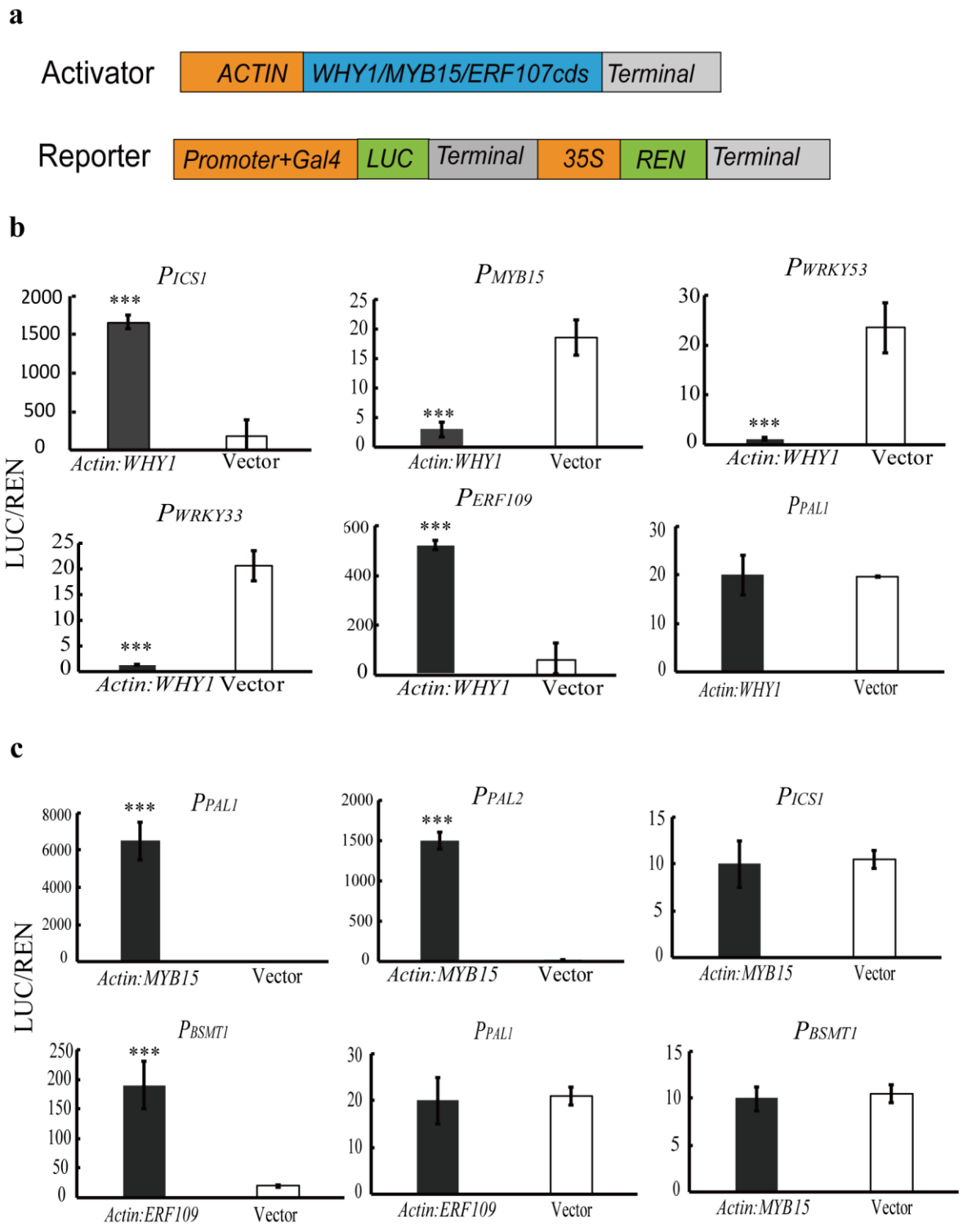

Figure 5. Promoter activation assays using the LUC/REN system

a. Structure of activator and reporter constructs. b. The promoters of *ICS1, MYB15, ERF109, WRKY53*, and *WRKY33* genes are co-infiltrated with a vector containing WHY1 under the regulation of the ACTIN promoter. c, Co-infiltration of MYB15 and

342 ERF109 with the *PAL1, PAL2, ICS1,* and *BSMT1* promoters. Background promoter
343 activity is assayed by co-infiltration with an empty vector of the same type. Shown are
344 means and SE of six biological replicates. Asterisks denote statistically significant
345 differences from the empty vector calculated using Student's t test: *, P, 0.05; **, P,
346 0.01; and ***, P, 0.001.

347 **WHY1 and MYB15/ERF109 regulate leaf senescence and ROS accumulation**

348 Since WHY1 is a repressor of plant senescence at early stage (35-42 dag) of plant
349 development (Miao et al. 2013), we compared the phenotype of the *pal1, sid2, myb15*,
350 *erf109* mutants (Supplementary Fig S2) with the *why1* mutant to analyze if WHY1
351 effects on salicylic metabolism impact senescence. The phenotypes of the *pal1* and
352 *sid2* plants have already been reported to delay senescence, and on the contrary,
353 *oePAL1*, *oeSID2* and *bsmt1* plants showed an early senescence phenotype (Love et
354 al., 2008; Rivas-San et al., 2011; Vlot et al., 2009; Huang et al. 2010). We analyzed all
355 mutants with respect to a visible senescent yellow leaf ratio (Miao and Zentgraf, 2007)
356 and reactive oxygen species (ROS) production by nitro blue tetrazolium chloride (NBT)
357 staining assay and diaminobenzidine (DAB) staining assay under normal growth
358 condition. The results showed that all of *pal1, sid2, myb15,* and *erf109* lines displayed
359 a visible delayed senescence and less ROS production except for the *bsmt1* plants,
360 which showed slightly earlier senescence and higher ROS accumulation similar to the
361 *why1* and the *pWHY1* lines (Figure 6a-b).

362 Furthermore, the transcript levels of senescence related genes *such as WRKY53,*
363 *SAG12, SAG13, SAG101,* and *PAD4* were measured by qRT-PCR and indicated as
364 heatmap (Figure 6c). They were upregulated in the *why1* and *pWHY1* plants，similar
365 to the overexpressing *PAL1* (*oePAL1)* plants, however downregulated in the *pal1*,
366 *myb15, and sid2* similar to the *nWHY1* plants (Figure 6c). Interestingly, in the
367 overexpressing *BSMT1 (oeBSMT1)* line the transcript level of senescence related
368 genes *SAG12* and *WRKY53* were upregulated, while the transcript level of *SAG13*
369 and *SAG101* were downregulated, a reversed expression trend as compared to the
370 *bsmt1* and *erf109* mutants (Figure 6c). However, the transcript level of *PAD4* was
371 upregulated in the both *bsmt1* and *oeBSMT1*. This indicates that BSMT1 is involved in
372 alternative signaling pathways between developmental senescence or stress related
373 senescence

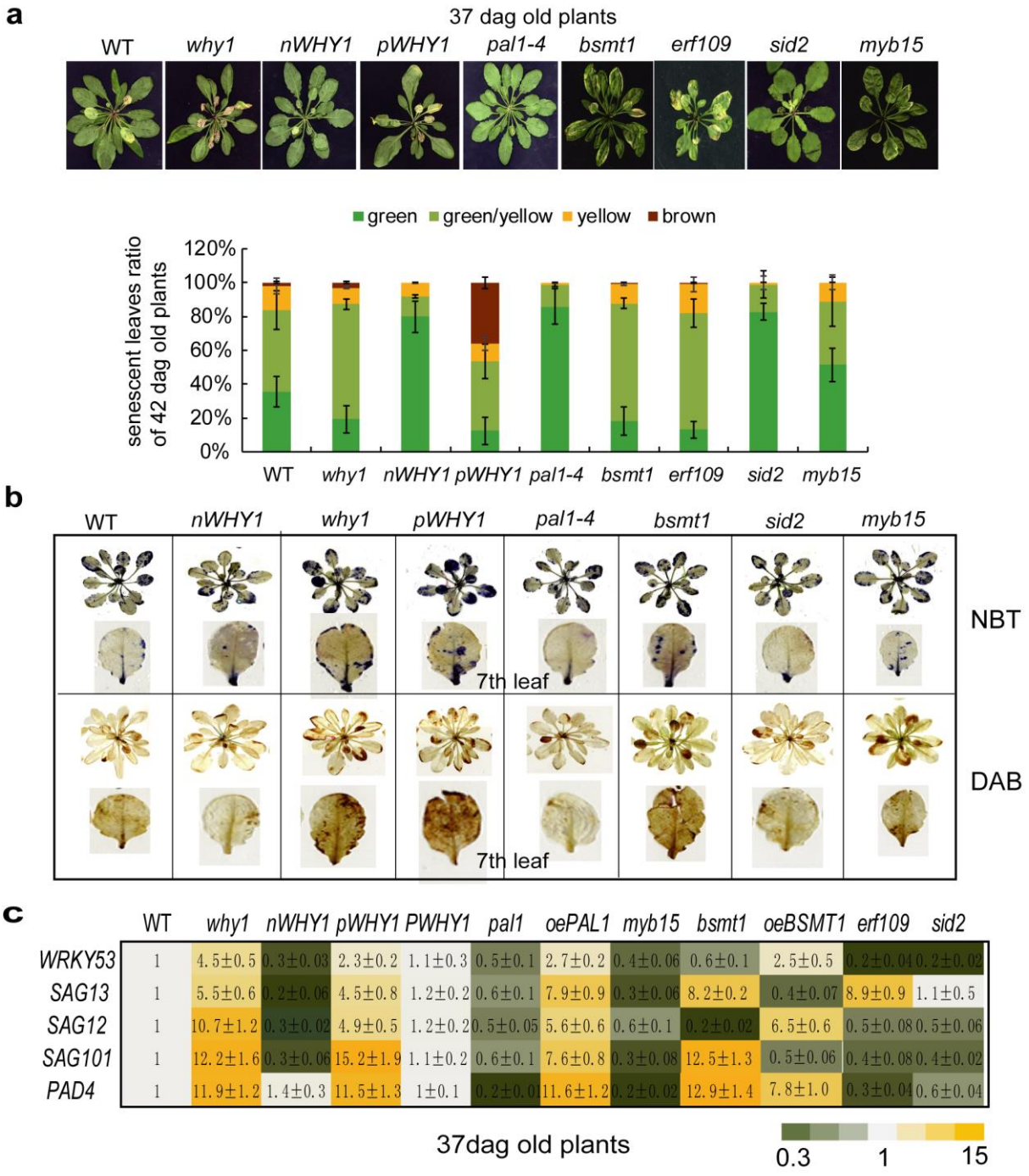

Figure 6. Phenotyping of loss- of *WHY1* and its downstream target genes mutants

a. Phenotypes of loss-of *PAL1, ICS1, MYB15* and *BSMT1* at 37dag compared to *WHY1* mutants. Whole rosette (a-up) and senescent leaf ratio of 5 plants (a-down); b. ROS accumulation of loss-of *PAL1, ICS1, MYB15* and *BSMT1* at 37dag compared to

379 *WHY1* mutants by NBT and DAB staining; c. The transcript levels of SAGs genes in
380 the loss- or gain- of *PAL1, BSMT1* and loss- of *MBY15, ERF109* and *ICS1* plants at
381 37dag by qRT-PCR. The standard error is calculated from three biological replicates,
382 the values are shown as means±SE. The wild-type at 37 dag was setup to 1 in the
383 heatmap.

384 **SA level feedback affects the distribution of the WHY1 protein in plastids and**
385 **the nucleus**

386 WHY1 is required for SA- and pathogen-induced *PR1* expression (Desveaux et al.
387 2005); WHY1 distribution is affected by protein modification (Ren et al. 2017) and
388 cellular H_2O_2 level (Lin et al. 2019). To determine whether SA feedback would affect
389 *WHY1* expression we quantified WHY1 transcription by qRT-PCR in response to
390 exogenous MeSA in WT plants for 1, 4, 6, and 8 hours. Unexpectedly, MeSA
391 treatment did not change the gene expression level of *WHY1* (Figure 7a). Thus, MeSA
392 treatment probably affects WHY1 protein function or distribution in plastids or the
393 nucleus. Thus, nuclear and plastid proteins isolated from 5-week-old WT rosettes
394 after MeSA treatment for 4 hours were immunodetected with a specific monoclonal
395 antibody against WHY1 (Lin et al. 2019; Supplementary Fig S4), and antibodies
396 against Histone 3 and photosystem II (PSII) protein were used as markers for pure
397 nuclear and plastid preparations (Figure 7b-c; Supplementary Fig S5). A water
398 treatment served as control for MeSA application. Interestingly, the results now
399 indicated that upon MeSA treatment for 4h, WHY1 accumulation significantly

400 decreases in plastids and the nuclear isoform of WHY1 was altered in its status with
401 small nWHY1 (29 kDa) levels slightly increasing, while large nWHY1 (37 kDa) levels
402 were decreasing after MeSA treatment (Figure 7b-c). Thus, exogenous MeSA
403 treatment affects WHY1 accumulation in plastids and alters the modification status of
404 nWHY1 in the nucleus, a similar response as observed in response to H_2O_2 treatment
405 (Lin et al. 2019). Furthermore, we analyzed WHY1 distribution between plastid and
406 nucleus under the condition of SA deficiency. The nuclear and plastid fractions
407 isolated from the single *sid2*, *pal1* mutants and double *sid2 pal1* mutant were
408 subjected to immunoblotting using the WHY1 specific peptide antibody and the results
409 demonstrate that pWHY1 in the *sid2*, *pal1* and *sid2 pal1* mutants significantly
410 accumulated in plastids when compared to WT. Accordingly, the large nuclear WHY1
411 isoforms (37 kDa) were highly accumulating and the small nuclear WHY1 proteins (27
412 kDa) were declining in the *sid2* and *sid2 pal1* mutants, but not in the *pal1* single
413 mutant (Figure b-d). This indicates that the ICS1 pathway plays a prominent role in
414 modification of nWHY1 protein.

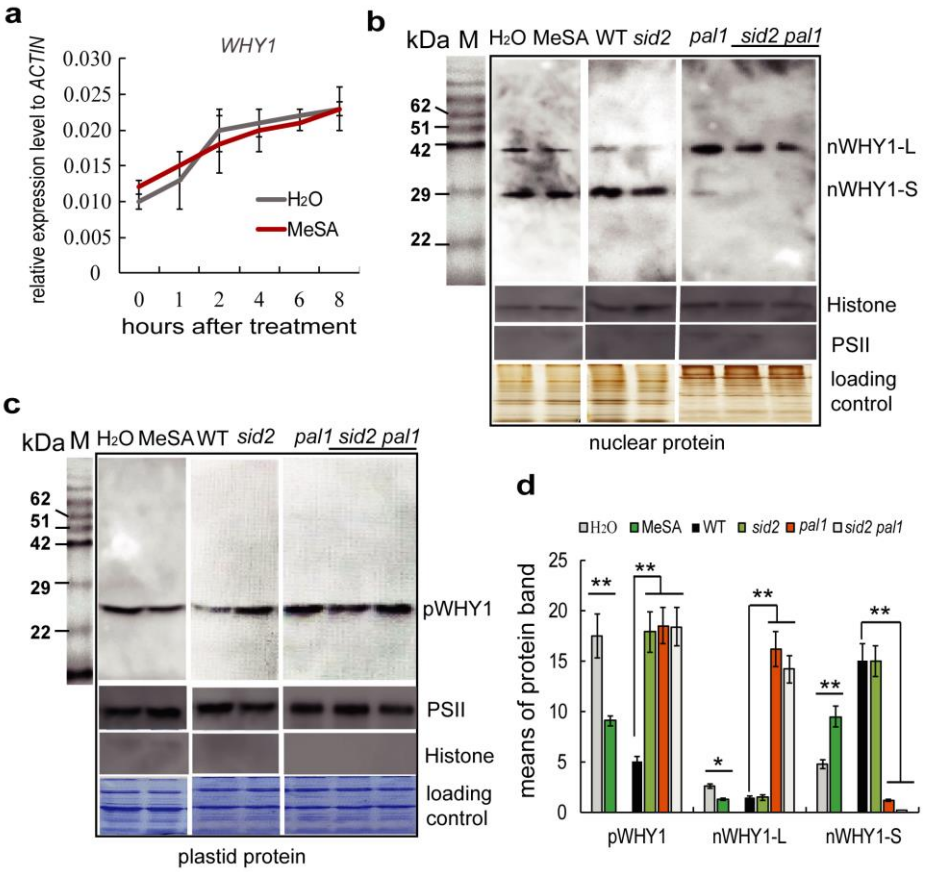

Figure 7. The plastid and nuclear isoform WHY1 protein immunodetection after the treatment of MeSA and in the *sid2, pal1* or double *sid2 pal1* mutants compared to WT a. The expression level of WHY1 in the WT plants after MeSA treatment for 1, 2, 4, 6, 8 hrs; b. WHY1 immunodetection in nuclear extracts after the treatment of MeSA for 4 hours, and in the *sid2, pal1* or double *sid2 pal1* mutants compared to WT; c. WHY1 immunodetection in plastid extracts after the treatment of MeSA for 4 hours, and in the *sid2, pal1* or double *sid2 pal1* mutants compared to WT. Coomassie and silver staining as the protein amount loading controls. L-WHY1: large size (37 kDa) of WHY1; S-WHY1: small size (29 kDa) of WHY1. The antibody against peptide WHY1 was prepared by company; d. The alteration of pWHY1 and nWHY1 after MeSA

426 treatment or in the sid2, pal1 or double sid2 pal1 mutants compared to WT. The
427 protein band signal is captured and calculated by Image J software program
428 (http://www.di.uq.edu.au/ sparqimagejblots). The data shows the average of three
429 replicates. Asterisks (*P < 0.05, **P < 0.01) show significant differences to H_2O
430 treatment or WT according to Student's t test.

431 Discussion

432 It has become increasingly clear that dual location of proteins mediates diverse
433 intercellular signaling processes, e.g. described for MAP kinase (Bobik et al. 2015;
434 Chan et al. 2016), CIPK14 (Ren et al. 2017), but also hormone (ABA, SA)
435 (Koussevitzky et al. 2007; Caplan et al. 2015; Kacprzak et al. 2019), or ROS
436 (hydrogen peroxidase and singlet oxygen) signaling (Lin et al. 2019; Duan et al. 2019,
437 Lv et al. 2019). Proteins with dual subcellular localization can affect transcription and
438 display various functions in intracellular signaling (Lin et al., 2019; Isemer et al., 2012;
439 Sun et al., 2011; Nevarez et al., 2017; Pesaresi and Kim, 2019; Wu et al., 2019;
440 Woodson et al., 2011/2013). This study revealed that dual-located WHY1 protein
441 directly activates *ICS1* expression in the nucleus at the late stage of plant
442 development, and indirectly controls PAL1 and BSTM1 expression *via* alteration of
443 *MYB15* and *ERF109* transcription at the early stage, thereby influencing the SA
444 homeostasis in the cells during plant development. A SA level feedback affects in turn
445 WHY1 distribution with a shift into the nucleus and preferential accumulation of the
446 smaller 29 kDa form. This loop of nWHY1 integrating SA homeostasis via PAL1/ICS1

447 and BSMT1 plays a pivotal role in controlling leaf senescence.

448 Elucidation of biosynthesis and catabolism of SA is important for understanding its
449 biological functions. 10% of SA is synthesized either from L-phenylalanine via the PAL
450 pathway in the cytoplasm or up to 90% from chorismate via ICS1/SID2
451 (ISOCHORISMATE SYNTHASE1/SALICYLIC ACID INDUCTION DEFICIENT2) in
452 chloroplasts, the latter of which is responsible for the bulk of SA produced during
453 pathogen infection in *Arabidopsis* (Dempsey et al. 2011). Endogenous SA can also
454 undergo a series of chemical modifications including hydroxylation by salicylate
455 hydroxylase (Yamamoto et al. 1965; Zhang et al., 2013), glycosylation by
456 glycosyltransferases (Lim et al. 2002; Dean et al. 2008), methylation by BSMT1 (Park
457 et al., 2007) and amino acid or sugar conjugation by XXX (Zhang et al., 2007; Bartsch
458 et al. 2010). The microarray data and qRT-PCR results show that the gene expression
459 levels of developmental related transcription factors were upregulated, and that of
460 stress-related gene were downregulated in the *why1* plants (Figure 3; supplementary
461 dataset 1-4). The expression levels of *ICS1, PAL1* and *BSMT1* were altered
462 significantly in the *why1* mutant during plant aging (Figure 1); this alteration can be
463 rescued completely by complementation of nWHY1 and pnWHY1 (Figure 2). As we
464 knew, nWHY1 could directly bind to the promoters of many targeted genes such as
465 *WRKY53*, *S40*, *Kenisin*, *PR10a* (Desveaux et al. 2005; Miao et al. 2013; Krupinska et
466 al. 2017; Xiong et al. 2009), as well as *MYB15*, *MYC1/2*, *ICS1* and several ERF family
467 members from our WHY1 ChIP-seq dataset (Figure 4; Miao et al., 2013). The nWHY1

468 represses most of downstream developmental related target gene expression such as
469 *WRKY53, WRKY33, MYB15, TTG2 etc.* (Figure 3; Supplementary dataset). However,
470 it can also promote expression of many stress-related genes such as *HvS40*
471 *(*Krupinska et al. 2013*), PR1* (Desveaux et al. 2005)*,* redox responsive transcription
472 factors (Foyer et al. 2014), *ICS1,* and *ERF109* (Figure 5; Figure 3; Supplementary
473 dataset). Several MYB family members can bind to the promoter of *PAL1/PAL2* (Battal
474 et al. 2019), and among these, MYB15 was shown to bind to the promoter of *PAL1*
475 and *ICE1* promoter by ChIP-qPCR. MYB15 mainly plays a virtual role in immunity and
476 cold response (Chezem et al. 2017; Kim et al. 2017; Wang et al. 2019). Our results
477 further confirmed that MYB15 could activate *PAL1* expression. ERF-binding cis
478 elements are enriched in the promoter region of *BSMT1*. However, *ERF109* as a
479 target gene of WHY1, which was identified in our ChIP-seq dataset (Miao et al. 2013;
480 Figure 4), was reported not to bind to the promoter region of *BSMT1* as shown in
481 yeast one hybrid and gel shift assays (Ximiao Shi, Master thesis, 2018). In contrast,
482 ERF109 can activate *BSMT1* expression in our LUC/REN transit assay (Figure 5),
483 supporting our ChIP-seq data. The *erf109* and *bsmt1* mutants accumulate high levels
484 of anthocyanin in response to high light (Foy et al. 2015), but the regulatory
485 mechanism is currently unknown. Therefore, the balance module of
486 nWHY1/MYB15-PAL1 and nWHY1/ERF109-BSMT1 at early stage (37 dag) and
487 WHY1/ICS1 regulation at late stage (42 dag) determines SA homeostasis during plant
488 development. The imbalance of PAL1/BSMT1 activity at 37 dag in the *why1* mutant

and repression of ICS1 at 42 dag of plant development may result in earlier SA accumulation for about one week. Thus, nWHY1 impacts the SA homeostasis *via* mediating PAL1 or ICS1 and BSMT1 activity in the cells during plant aging.

The WHIRLY family is considered to associate with retrograde signaling. Due to their dual-location and function in the nucleus and plastids (Krause et al., 2009), it has been supposed that WHIRLY1 could move from plastid to the nucleus (Isemer et al., 2012). The plastid isoform of WHIRLY1 affects the *miRNA* biogenesis in the nucleus (Swida-Barteczka et al. 2018). Previously, we showed that the WHY1 protein can be phosphorylated by CIPK14 kinase or oxidized by H_2O_2, leading to different subcellular localization in the nucleus or in plastids, respectively (Ren et al. 2017; Lin et al. 2019). Here, we show that loss- of WHY1 results in five days earlier SA production during plant development, thereby accelerating plant senescence. Complementation with pWHY1, did not revert the SA accumulation phenotype. On the contrary, the pWHY1 further increased SA accumulation during plant development. Consistently, gene expression of *PAL1* is promoted, while that of *BSMT1* is repressed at 37 dag, while ICS1 is activated at 42 dag (Figure 1). This phenomenon can be explained by two mechanisms: 1) H_2O_2 is known to affect SA levels via the ICS1 pathway (Leon et al. 1995; Dat et al. 1998; Chaouch et al. 2010; Guo et al. 2017) and recent data link pWHY1 to ROS production *via* photosystem I/II (PSI/PSII) (Huang et al. 2017; Lin et al. 2019). Thus, pWHY1 might increase SA level at 42 dag by modulation of the ICS1 pathway via photosystem induced ROS accumulation to cause an early senescent

phenotype. 2) pWHY1 coordinating SA homeostasis is feedback controlled by cellular SA levels ((Desveaux et al. 2005; Isemer et al. 2012; Caplan et al. 2017), so this WHY1 isoform changes from plastid to nucleus repressing *MYB15* and *PAL1* expression (Huang et al. 2010; Duan et al., 2019) and activating *ERF109* and *BSMT1* expression in response to stress cues such as high light (Estavillo et al. 2011). This demonstrates that dual located pWHY1/nWHY1 affects SA homeostasis most likely *via* connection with PSI/II mediated ROS affecting leaf senescence.

The distribution of WHY1 between plastids and the nucleus depends not only on its modification status (Ren et al. 2017) but also on environmental cues or cellular signals such as H_2O_2 (Lin et al. 2019) and SA (this work). Though, the SA signal cannot promote CIPK14 expression (unpublished data), MeSA treatment feedback alters the nWHY1 protein status (37 kDa or 29 kDa form) (Figure 7) similar to barley WHY1 (Grabowski et al. 2008) and nWHY1 after treatment with H_2O_2 in *Arabidopsis* (Lin et al. 2019). The nature of modification resulting in both forms is yet unknown and has to be revealed in future. More interestingly, MeSA treatment reduced WHY1 accumulation in plastids, which stands in contrast to H_2O_2 treatment (Lin et al. 2019). These phenomena are further elucidated in the SA deficient mutants such as *pal1, sid2* and double *pal1 sid2* mutants. Loss-of ICS1 (*sid2*) decreases the modified state of nWHY1 level, while loss-of ICS1 or PAL1 increases WHY1 accumulation in plastids. It is known that ICS1 is located in plastids and is responsible for the bulk production of SA in response to salt or pathogens (Kumazaki and Suzuki, 2019). Plastid-derived SA

can be transported from plastid to the nucleus *via* stromule (Caplan et al. 2015). It is speculated that this kind of SA might influence the nuclear isoform of WHY1, which small form (29 kDa) activates the stress related gene expression, such as *S40*, *ICS1* (Krupinska et al., 2013; Figure 4-5), while the large form (37 kDa) represses gene expression, as shown for *WRKY53, WRKY33, MYB15* (Miao et al. 2013; Figure 4-5). Furthermore, it has been reported that phosphorylation of WHY1 by CIPK14 promoted its binding affinity at the promoter of *WRKY53* and *WRKY33* and repressed *WRKY53* and *WRKY33* expression (Ren et al. 2017) and that CIPK kinase expression level rapidly increased in response to salt or pathogen, accompanying increasing Ca^{2+}, H_2O_2 and SA levels in the cells (Sardar et al., 2017).

Conclusion

We conclude that WHY1 exerts dual functions in plastids and the nucleus. Nuclear WHY1 maintains SA homeostasis by directly affecting *ICS1* and indirectly affecting *PAL1* and *BSTM1* expression via *MYB15* and *ERF109*. The pWHY1 isoform promotes PAL1/ICS1 expression and represses BSMT1 facilitating high SA accumulation, resulting in early senescence, similar to *bsmt1* mutants. Interestingly, MeSA treatment altered the nWHY1 status (increasing the 29 kDa form of WHY1, while decreasing the 37 kDa form), going along with declined pWHY1 accumulation. These results indicate that pWHY1/nWHY1 distribution in the nucleus and chloroplast allows balancing SA and H_2O_2 homeostasis, in a developmental dependent manner, thereby affecting leaf senescence in *Arabidopsis* (Figure 8).

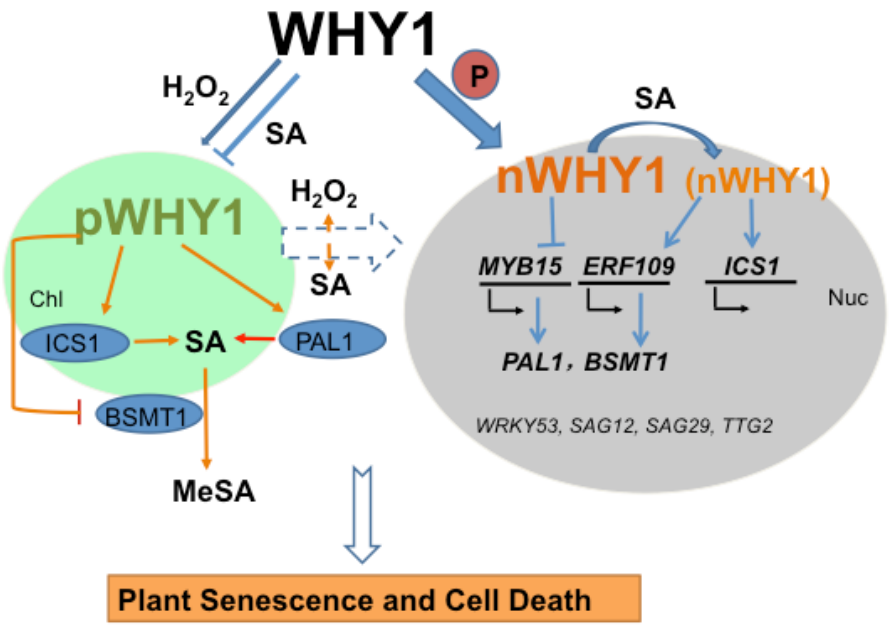

552

553 Figure 8. A working model of the senescence pathway performed by the dual located
554 WHY1 in response to SA. The nuclear isoforms of WHY1 are represented as both a
555 large molecular mass (37 kDa, bigger letters in the Figure) and a small molecular
556 mass (29 kDa, smaller letters). WHY1 has dual functions in plastids and the nucleus.
557 Loss of WHY1 increases SA accumulation at early stage (37 dag) through increasing
558 PAL1 expression and repressing BSMT1; Elevated SA promotes nuclear WHY1
559 de-modification and promotes ICS1 and BSMT1 expression thereby balancing SA
560 homeostasis in the cells. High SA levels by ICS1 cause feedback enhancing ROS
561 accumulation, promoting senescence. pWHY1 stimulates PAL1/ICS1 expression but
562 represses BSMT1, allowing high levels of SA, leading also to early senescence. Thus,
563 distribution of WHY1 organelle isoforms and the putative feedback of SA form a
564 circularly integrated regulatory network during plant senescence in a developmental
565 dependent manner. Plastid (Chl) is shown as a green ovary, nucleus (Nuc) as a grey

566 ovary, lines for regulation, fat arrows for transfer or translocation, broken lines for
567 uncertainty.

568 Materials and Methods

569 Plant materials

570 All *Arabidopsis thaliana* mutants are in Col-0 background. The T-DNA insertion
571 lines *why1* (Salk_023713), *sid2*, *pal1*, *bsmt1* (SAIL_776_B10), *myb15* (*myb15-1*
572 SALK_151976, *myb15-2* SK2722) were kindly provided by other scientists; The
573 *erf109* (SALK_150614) and over-expression lines of ERF109 gene (CS2102255)
574 were obtained from the Nottingham Arabidopsis stock center (NASC). Homozygous
575 plants were selected and confirmed by PCR or RT-PCR using gDNA and mRNA as
576 templates (Supplementary Fig S2), respectively (http://signal.salk.edu/
577 tdnaprimers.2.html). The overexpressing *nWHY1-HA* lines that produce the WHY1
578 protein located only in the nucleus, the overexpressing *pnWHY1-HA* lined that
579 produce the WHY1 protein dually located in plastids and the nucleus, the complement
580 *PWHY1-HA* (*Pwhy1:pnWHY1-HA*) line, and the *pWHY1-HA* lines that harbor the
581 construct of the full length WHY1 plus nuclear export peptide sequence fused to
582 HA-tag produces WHY1 protein located only in plastids have been constructed in our
583 lab (Miao et al. 2013; Lin et al. 2019).

584 Seeds are germinated on wet filter paper followed by vernalization at 4°C for 2 d,
585 then transplanted to vermiculite and are grown in a climatic chamber (100 μE/h, 13h
586 of light at 22°C/11h of dark at 18°C, 60% relative humidity). The rosette leaves are

587 labeled with colored threads after emergence, as described previously (Hinderhofer
588 and Zentgraf 2001).

589 For MeSA treatment, rosette leaves are collected at 1, 2, 4, 6, and 8 hours after
590 spraying with 100 μM MeSA and stored in liquid nitrogen or -80 °C for later use in RNA
591 or protein isolations. Mock treatments used distilled water instead.

592 Measurement SA contents in rosette leaves

593 SA was extracted from 0.2 g the 5th leaf from individual plants at different stages of
594 development and measured by reversed-phase high-performance liquid
595 chromatography (HPLC) on an Agilent1260 system with a C18 column as previously
596 described (Verberne et al. 2002) with small modifications: SA was thoroughly
597 separated from the complex mixture by methanol containing 10% of sodium acetate
598 with pH 6.0 (Lin et al. 2017). Fluorescence detection (excitation at 305 nm and
599 emission at 407 nm) was applied and 3-Hydroxybenzoic acid (3-HBA) was used as an
600 internal standard (Aboul-Soud et al. 2004). Conjugated and free SA was detected at
601 the same time. Three independent biological replicates were performed for each data
602 point.

603 Staining of ROS

604 Visualization of H_2O_2 accumulation in leaves was performed using the
605 3',3'-diaininobenzidine (DAB) staining method according to Zhang et al. (2014) and
606 Huang et al. (2019). Detached rosette leaves were vacuum filtered in 20 mL staining
607 solution containing 1 mg/mL DAB in 50 mM Tris-HCl, pH 5.0 for 10 min, and incubated

608 in the darkness at room temperature for 12 h. The leaves were destained by boiling in
609 a mixture of ethanol, glycerol and acetic acid (3/1/1, v/v/v) for 15 min before imaging.
610 Detection of superoxide free radicals were performed by the nitroblue tetrazolium
611 (NBT) staining method as described in Lee et al. (2002). The whole rosette leaves of
612 5- to 6-week-old plants were harvested and immersed in 0.1 mg ml-1 NBT solution (25
613 mM HEPES, pH7.6). After vacuum infiltration, samples were incubated at 25°C for 2 h
614 in the darkness. Subsequently stained samples were bleached in 70% ethanol and
615 incubated further for 24 h at 25°C to remove the chlorophyll.

616 Imaging was conducted using an Epson Perfection V600 Photo scanner (Epson
617 China, Beijing, China).

618 Quantitative real-time PCR analysis (qRT-PCR)

619 The qRT-PCR was performed using SYBR Green master mix (SABiosciences,
620 Frederick, MD, USA) according to the manufacturer's instructions. Complementary
621 DNA synthesis was carried out using a Fermentas first-strand complementary DNA
622 synthesis kit (Thermo Fisher Scientific, Waltham, MA, USA) on RNA from
623 28-55-day-old plants grown under normal light conditions. Complementary DNAs
624 were diluted 20-fold prior to quantitative PCR experiments. The Touch 1000 platform
625 (Bio-Rad) was used for qRT-PCR experiments, and the data were analyzed using
626 Bio-Rad software version 1.5. We used *GAPC2* or *ACTIN* as internal reference genes
627 for calculation of relative expression. Primers are listed in Supplemental Table S1. All

628 determinations were conducted in three biological replicates.

629 Isolation and detection of plastid and nuclear proteins

630 Chloroplasts and nuclei were prepared and purified as described previously (Ren et al.
631 2017). Approximately 10 microgram proteins of each fraction was separated on 14%
632 (w/v) polyacrylamide gels. After transfer to nitrocellulose membranes,
633 immunodetection followed using specific antibodies against the WHY1 C-terminal
634 peptide CASPNYGGDYEWNR (Faan, Hangzhou, China). To monitor the purity of the
635 chloroplast and nuclear fractions, we used antibodies against the cytochrome b559
636 apoprotein A or the histone H3 (Cell Signaling, Munich, Germany), respectively (Lin et
637 al. 2019).

638 ChIP-qPCR assay

639 Four-week-old rosettes of transgenic plants expressing the *Pwhy1:WHY1-HA* to
640 complement the *why1* knockout background were used for sample preparations. The
641 cross-linked DNA fragments ranging from 200 to 1000 bp in length were
642 immunoprecipitated by an antibody against the HA-tag (Cell Signaling, Munich,
643 Germany). The enrichments of the selected promoter regions of both genes were
644 resolved by comparing the amounts in the precipitated and non-precipitated (input)
645 DNA samples, which were quantified by quantitative PCR using designed
646 region-specific primers (Supplementary Table S1 and Figure 4). Material from the
647 *why1* mutant served as a mock control and was used for normalizations to calculate
648 the fold enrichment. The experiments were performed three times biological

649 replicates.

650 Cloning and Construction of Vectors

651 The promoter sequences of 2kb upstream of ATG of *MYB15* and the *ERF109,*
652 *WRKY53, PAL1, PAL2, ICS1*, and *WRKY33* genomic sequence were PCR-amplified
653 and then restricted with *Kpn*I and *Xho*I, or *Xho*I and *Pst*I respectively and sub-cloned
654 into the pFLAP vector The entire cassette was then excised with *Kpn*I and *Asc*I and
655 cloned into the binary vector pBIN +.

656 For dual Luciferase assays, promoter sequences were PCR-amplified, digested with
657 *Nco*I and *Kpn*I and cloned into the pGreenII 0800-LUC binary vector (provided by
658 Roger P. Hellens). DNA constructs used for *N. benthamiana* agro-infiltration and for
659 agrobacteria-mediated plant transformation were constructed with the Goldenbraid
660 cloning (Sarrion Perdigones et al., 2013).

661 *MYB15*, *ERF109* and *WHY1* coding sequences were subcloned into a pUPD vector.
662 In the dual Luciferase assays; MYB15, ERF109, and WHY1 were in the 1α1 vectors
663 which are based on a pGREENII backbone. For generating the genes overexpression
664 construct, a CDS fragment was amplified subcloned into pGEM-T Easy (Promega),
665 excised with *Bam*HI and *Sal*I restriction enzymes and cloned under the CaMV-35S
666 promoter into pFLAP, before restriction with *Pac*I and *AscI* and ligation to the pBIN+
667 binary vector.

668 Dual-luciferase activity assay

669 *Nicotiana benthamiana* plants were grown in climate rooms (22°C, 16/8 h of

light/dark). Plants were grown until they had six leaves and then infiltrated with *Agrobacterium tumefaciens GV3101*. Plants were maintained in the climate rooms and, after 4 to 5 d, 1-cm discs were collected from the fourth and fifth leaves of each plant. Six biological replicates with their respective negative controls were used per assay. The experiment was performed as previously described (Hellens et al., 2005) with minor changes. Agrobacterium was grown over night in LB and brought to a final O.D.600 0.2 in infiltration buffer. Co-infiltrated Agrobacterium carried separate plasmids; 900 µl of an empty cassette or one that contains the transcription factor driven by the tomato 2 kb UBQ10 (SOLYC7G064130) promoter region, and 100 µl of the reporter cassette carrying one of the test promoters. Leaf discs were homogenized in 300 µl of a passive lysis buffer. 25 µl of a 1/100 dilution of the crude extract was assayed in 125 µl of Luciferase assay buffer, and LUC and REN chemiluminescence of each sample was measured in separate wells on the same plate. RLU were measured in a Turner 20/20 luminometer, with a 5 seconds delay and 15 seconds measurement. Raw data was collected and the LUC/REN ratio was calculated for each sample. Biological samples were polled together and a student's t-test was performed against a background control for each experiment as described in the results section. The entire experiment was repeated a second time under similar conditions to confirm the regulatory effect of transcription factors.

Microarray Analysis

Two biological replicates were sampled from leaves of wild-type, *VEX:pWHY1/why1*，

691 *VEX：nWHY1/why1*, and the *why1* plants (see our previous paper Ren et al. 2017).
692 Extracted RNA was then amplified and labeled using the standard Affymetrix protocol
693 and hybridized to Affymetrix ATH1 GeneChips according to the manufacturer's
694 guidelines (Katari et al. 2010). Statistical analysis of transcriptome data was carried
695 out using Parke Genome Suite software (www.partek.com). Data preprocessing and
696 normalization were performed using the Robust Microarray Averaging algorithm
697 (Irizarry et al., 2003). Batch effects between the replicates were not found.
698 Differentially expressed genes were identified by using ANOVA according to false
699 discovery rate, p-value 0.05 and at least a 2-fold change between the genotypes
700 (Supplementary Dataset 1-4).

701 Statistical analysis

702 Quantitative data were determined by at least three biological replicates and the
703 statistical significance was analyzed either using two-way ANOVA or pair-wide
704 multiple t-tests, with the GraphPad Prism software (version 7).

705 Acknowledgments

706 We acknowledge Dr. Hongwei Guo (University of Southern Technology) for providing
707 the *sid2*, Dr. Zhixiang Chen (Purdue University) for providing the *pal1-4* seeds, Dr.
708 Nicola Clay (Yale University) for providing the seed of *oeMYB15* and the *myb15*, Dr.
709 Daniel Klessig (University of California, Berkeley) for providing the *bsmt1* seeds. We
710 acknowledge the European Arabidopsis Stock Centre providing series of Arabidopsis
711 mutant seeds (*oe:ERF109* and *erf109* lines). This work is supported by a grant from

712 the Natural Science Foundation of China (NSFC, No. 31770318, 31470383), and by a
713 grant from Fujian Provincial NSF (No. 2016J01103), and by a grant of international
714 exchange program of Fujian Agriculture and Forestry University (KXB16009A).

715 Author contributions

716 Y.M. designed the study. W.F.L. performed SA measurements, western blots,
717 phenotyping, and qRT-PCR. D.H. performed ChIP-seq, ChIP-qPCR. H.Z. performed
718 plasmid constructs and promoter activation activity and the mutants screening. B.H.W
719 performed microarray data analyses. W.F.L. and Y.M. analyzed the data. Y.M. and D.S.
720 wrote the paper. D.C. critically read the paper.

721 Competing interests

722 The authors declare no competing interests.

723 Supporting information:

724 Supplementary Fig S1 Transcript levels of *ICS2*, *UGT71B1, UGT89B1*, *UGT74F2* and
725 *S3H* in the *why1* mutant compared to WT during plant aging

726 Supplementary Fig S2 Verification of mutant plants used in this study..

727 Supplementary Fig S3 Venn analysis of transcriptome of nWHY1, pWHY1, pnWHY1
728 and *why1*

729 Supplementary Fig S4 Antibody specificity test.

730 Supplementary Fig S5 Western blot detection to certify purity of nuclear protein and
731 plastid protein extracts.

732 Supplementary Table S1. The list of primer sequences for PCR in this study

733 Supplementary dataset 1-4

734

735 References

736 Aboul-Soud MAM, Cook K, Loake GJ (2004) Measurement of Salicylic Acid by a
737 High-Performance Liquid Chromatography Procedure Based on Ion-Exchange.
738 Chromatographia 59: 129-133

739 Alonso-Ramírez A, Rodríguez D, Reyes D, Jiménez JA, Nicolás G, López-Climent M,
740 Gómez-Cadenas A, Nicolás C (2009) Evidence for a role of gibberellins in salicylic
741 acid-modulated early plant responses to abiotic stress in Arabidopsis seeds. Plant
742 Physiol. 150(3):1335-44.

743 An C, Mou Z (2011) Salicylic acid and its function in plant immunity. J Integr Plant Biol
744 53: 412-428

745 Bartsch M, Bednarek P, Vivancos PD, Schneider B, von Roepenack-Lahaye E, Foyer
746 C, Kombrink E, Scheel D (2010) Accumulation of isochorismate-derived
747 2,3-dihydroxybenzoic 3-O-beta-D-xyloside in arabidopsis resistance to pathogens
748 and ageing of leaves. J Biol Chem 285(33):25654–25665.

749 Battat M, Eitan A, Rogachev I, Hanhineva K, Fernie A, Tohge T, Beekwilder J, and
750 Aharoni A (2019) A MYB Triad Controls Primary and Phenylpropanoid Metabolites
751 for Pollen Coat Patterning. Plant Physiol, 180, 87–108,

752 Bobik K, and Burch-Smith T (2015) Chloroplast signaling within, between and beyond

753 cells. Front. Plant Sci. 6:781

754 Caplan JL, Kumar AS, Park E, Padmanabhan MS, Hoban K, Modla S, Czymmek K, S.
755 Dinesh-Kumar P (2015) Chloroplast stromules function during innate immunity. Dev
756 Cell 34(1): 45–57

757 Cappadocia L, Marechal A, Parent JS, Lepage E, Sygusch J, Brisson N (2010)
758 Crystal structures of DNA-Whirly complexes and their role in Arabidopsis organelle
759 genome repair. Plant Cell 22: 1849-1867

760 Cappadocia L, Parent JS, Zampini E, Lepage E, Sygusch J, Brisson N (2012) A
761 conserved lysine residue of plant Whirly proteins is necessary for higher order
762 protein assembly and protection against DNA damage. Nucleic Acids Res 40:
763 258-269

764 Chan KX, Phua SY, Crisp P, McQuinn R, Pogson, BJ (2016). Learning the languages
765 of the chloroplast: Retrograde signaling and beyond. Annu. Rev. Plant Biol. 67: 25–
766 53.

767 Chaouch S, Queval G, Vanderauwera S, Mhamdi A, Vandorpe M, Langlois-Meurinne
768 M, Van Breusegem F, Saindrenan P, Noctor G. (2010) Peroxisomal hydrogen
769 peroxide is coupled to biotic defense responses by ISOCHORISMATE
770 SYNTHASE1 in a daylength-related manner. Plant Physiol. 2010 153(4):1692-705.

771 Chezem WR, Memon A, Li FS, Weng JK, Clay NK. (2017) SG2-Type R2R3-MYB
772 Transcription Factor MYB15 Controls Defense-Induced Lignification and Basal
773 Immunity in Arabidopsis. Plant Cell 29(8):1907-1926

774 Comadira G, Rasool B, Kaprinska B, Garcia BM, Morris J, Verrall SR, Bayer M,
775 Hedley PE, Hancock RD, Foyer CH (2015) WHIRLY1 Functions in the Control of
776 Responses to Nitrogen Deficiency But Not Aphid Infestation in Barley. Plant Physiol
777 168: 1140-1151
778 Dat JF, Lopez-Delgado H, Foyer CH, Scott IM (1998) Parallel changes in H2O2 and
779 catalase during thermotolerance induced by salicylic acid or heat acclimation in
780 mustard seedlings. Plant Physiol 116: 1351-1357
781 Dean JV, Delaney SP (2008) Metabolism of salicylic acid in wild-type, ugt74f1 and
782 ugt74f2 glucosyltransferase mutants of Arabidopsis thaliana. Physiol Plant
783 132(4):417–425.
784 Dempsey DA, Vlot AC, Wildermuth MC, Klessig DF (2011) Salicylic Acid biosynthesis
785 and metabolism. Arabidopsis Book 9: e0156
786 Desveaux D, Despres C, Joyeux A, Subramaniam R, Brisson N (2000) PBF-2 is a
787 novel single-stranded DNA binding factor implicated in PR-10a gene activation in
788 potato. Plant Cell 12: 1477-1489
789 Desveaux D, Marechal A, Brisson N (2005) Whirly transcription factors: defense gene
790 regulation and beyond. Trends Plant Sci 10: 95-102
791 Desveaux D, Subramaniam R, Despres C, Mess JN, Levesque C, Fobert PR, Dangl
792 JL, Brisson N (2004) A "Whirly" transcription factor is required for salicylic
793 acid-dependent disease resistance in Arabidopsis. Dev Cell 6: 229-240
794 Duan J, Lee KP, Dogra V, Zhang S, Liu K, Caceres-Moreno C, Lv S, Xing W, Kato Y,

795 Sakamoto W, Liu R, Macho AP, Kim C (2019) Impaired PSII Proteostasis Promotes
796 Retrograde Signaling via Salicylic Acid. Plant Physiol 180(4):2182-2197
797 Estavillo GM, Crisp PA, Pornsiriwong W, Wirtz M, Collinge D, Carrie C, Giraud E,
798 Whelan J, David P, Javot H, Brearley C, Hell R, Marin E, Pogson BJ (2011)
799 Evidence for a SAL1-PAP chloroplast retrograde pathway that functions in drought
800 and high light signaling in Arabidopsis. Plant Cell 23: 3992-4012
801 Foyer CH, Karpinska B, Krupinska K (2014) The functions of WHIRLY1 and
802 REDOX-RESPONSIVE TRANSCRIPTION FACTOR 1 in cross tolerance
803 responses in plants: a hypothesis. Philos Trans R Soc Lond B Biol Sci 369:
804 20130226
805 Friedrich L, Vernooij B, Gaffney T, Morse A, Ryals J (1995) Characterization of
806 tobacco plants expressing a bacterial salicylate hydroxylase gene. Plant Mol Biol
807 29(5):959–968.
808 Gawroński P, Górecka M, Bederska M, Rusaczonek A, Ślesak I, Kruk J, Karpiński S.
809 (2013) Isochorismate synthase 1 is required for thylakoid organization, optimal
810 plastoquinone redox status, and state transitions in Arabidopsis thaliana. J Exp Bot
811 64(12):3669-79..
812 Garcion C, Lohmann A, Lamodière E, Catinot J, Buchala A, Doermann P, Métraux JP
813 (2008) Characterization and biological function of the ISOCHORISMATE
814 SYNTHASE2 gene of Arabidopsis. Plant Physiol 147(3):1279–1287.
815 Grabowski E, Miao Y, Mulisch M, Krupinska K (2008) Single-stranded DNA-binding

protein Whirly1 in barley leaves is located in plastids and the nucleus of the same cell. Plant Physiol 147: 1800-1804

Guo P, Li Z, Huang P, Li B, Fang S, Chu J, Guo H.(2017) A Tripartite Amplification Loop Involving the Transcription Factor WRKY75, Salicylic Acid, and Reactive Oxygen Species Accelerates Leaf Senescence. Plant Cell 29(11):2854-2870.

Hellens RP, Allan AC, Friel EN, Bolitho K, Grafton K, Templeton MD, Karunairetnam S, Gleave AP, Laing WA (2005) Transient expression vectors for functional genomics, quantification of promoter activity and RNA silencing in plants. Plant Methods 1: 13

Hinderhofer K, Zentgraf U (2001) Identification of a transcription factor specifically expressed at the onset of leaf senescence. Planta 213: 469-473

Huang D, Lin W, Deng B, Ren Y, Miao Y (2017) Dual-Located WHIRLY1 Interacting with LHCA1 Alters Photochemical Activities of Photosystem I and Is Involved in Light Adaptation in Arabidopsis. Int J Mol Sci 18

Huang J, Gu M, Lai Z, Fan B, Shi K, Zhou YH, Yu JQ, Chen Z (2010) Functional analysis of the Arabidopsis PAL gene family in plant growth, development, and response to environmental stress. Plant Physiol 153: 1526-1538

Huang L, Yu LJ, Zhang X, Fan B, Wang FZ, Dai YS, Qi H, Zhou Y, Xie LJ, Xiao S (2019) Autophagy regulates glucose-mediated root meristem activity by modulating ROS production in Arabidopsis. Autophagy 15: 407-422

Irizarry RA, Hobbs B, Collin F, Beazer-Barclay YD, Antonellis KJ, Scherf U, Speed TP (2003) Exploration, normalization, and summaries of high density oligonucleotide

837 array probe level data. Biostatistics 4: 249–264

838 Isemer R, Mulisch M, Schafer A, Kirchner S, Koop HU, Krupinska K (2012)
839 Recombinant Whirly1 translocates from transplastomic chloroplasts to the nucleus.
840 FEBS Lett 586: 85-88

841 Kacprzak SM, Mochizuki N, Naranjo B, Xu D, Dario Leister D, Kleine T, Okamoto H,
842 Terry MJ (2019) Plastid-to-Nucleus Retrograde Signalling during Chloroplast
843 Biogenesis Does Not Require ABI4. Plant Physiol 179:18–23

844 Katari MS, Nowicki SD, Aceituno FF, Nero D, Kelfer J, Thompson LP, Cabello JM,
845 Davidson RS, Goldberg AP, Shasha DE, Coruzzi GM, Gutiérrez RA (2010)
846 VirtualPlant: A Software Platform to Support Systems Biology Research Plant
847 Physiol 152, 500–51.

848 Kim SH, Kim HS, Bahk S, An J, Yoo Y, Kim JY, Chung WS (2017) Phosphorylation of
849 the transcriptional repressor MYB15 by mitogen-activated protein kinase 6 is
850 required for freezing tolerance in Arabidopsis. Nucleic Acids Res 45(11):6613-6627

851 Kleine T, Leister D (2016) Retrograde signaling: Organelles go networking. Biochim
852 Biophys Acta 1857: 1313-1325

853 Kleine T, Voigt C, Leister D (2009) Plastid signalling to the nucleus. Trends Genet 25:
854 185-192

855 Kong F, Zhang S, Yang M, Liu Z, Wang Y, Ma N. Meng Q. (2018) Whirly1 enhances
856 the tolerance to chilling stress in tomato via protection of Photosystem II and
857 regulation of starch degradation. New Phytologist

858 Koussevitzky S, Nott A, Mockler TC, Hong F, Sachetto-Martins G, Surpin M, Lim J,
859 Mittler R, Chory J (2007) Signals from chloroplasts converge to regulate nuclear
860 gene expression. Science 316: 715-719
861 Krause K, Kilbienski I, Mulisch M, Rodiger A, Schafer A, Krupinska K (2005)
862 DNA-binding proteins of the Whirly family in Arabidopsis thaliana are targeted to
863 the organelles. FEBS Lett 579: 3707-3712
864 Krause K, Krupinska K (2009) Nuclear regulators with a second home in organelles.
865 Trends Plant Sci 14: 194-199
866 Krupinska K, Dähnhardt D, Fischer-Kilbienski I, Kucharewicz W, Scharrenberg C,
867 Trösch M, Buck F (2013) Identification of WHIRLY1 as a Factor Binding to the
868 Promoter of the Stress- and Senescence-Associated Gene HvS40. J of Plant
869 Growth Reg 33: 91-105
870 Kucharewicz W, Distelfeld A, Bilger W, Müller M, Munné-Bosch S, Hensel G,
871 Krupinska K (2017) Acceleration of leaf senescence is slowed down in transgenic
872 barley plants deficient in the DNA/RNA-binding protein WHIRLY1. J of Exp Bot 68(5)
873 983–996
874 Kumazaki A, Suzuki N. (2019) Enhanced tolerance to a combination of heat stress
875 and drought in Arabidopsis plants deficient in ICS1 is associated with modulation of
876 photosynthetic reaction center proteins. Physiol Plant 165(2):232-246.
877 Lee BH, Lee H, Xiong L, Zhu JK. (2002) A mitochondrial complex I defect impairs
878 cold-regulated nuclear gene expression. Plant Cell 14: 1235–1251

879 Lee S, Kim SG, Park CM (2010) Salicylic acid promotes seed germination under high
880 salinity by modulating antioxidant activity in Arabidopsis. New Phytol 188: 626-637
881 Lescot M, Deohais P, Thijs G, Marchal K, Moreau Y, Van de Peer Y, Rouz P and
882 Rombauts S. (2002) PlantCARE, a database of plant cis-acting regulatory
883 elements and a portal to tools for in silico analysis of promoter sequences. Nucleic
884 Acids Res 30(1):325-327
885 Leon J, Lawton MA, Raskin I (1995) Hydrogen Peroxide Stimulates Salicylic Acid
886 Biosynthesis in Tobacco. Plant Physiol 108: 1673-1678
887 Leon J, Shulaev V, Yalpani N, Lawton MA, Raskin I (1995) Benzoic acid
888 2-hydroxylase, a soluble oxygenase from tobacco, catalyzes salicylic acid
889 biosynthesis. Proc Natl Acad Sci U S A 92: 10413-10417
890 Lepage E, Zampini E, Brisson N (2013) Plastid genome instability leads to reactive
891 oxygen species production and plastid-to-nucleus retrograde signaling in
892 Arabidopsis. Plant Physiol 163: 867-881
893 Lim EK, Doucet CJ, Li Y, Elias L, Worrall D et al. (2002) The activity of Arabidopsis
894 glycosyltransferases toward salicylic acid, 4-hydroxybenzoic acid, and other
895 benzoates. J Biol Chem 277(1):586–592.
896 Lin W, Zhang H, Hong Z, Miao Y, Lin W (2016) A general method for detection the
897 content of endogenous salicylic acid in plant leaf by HPLC. J Fujian Agri & Fore Uni
898 46:109-114
899 Lin W, Huang D, Shi X, Deng B, Ren Y, Lin W, Miao Y, (2019) H2O2 as a Feedback

900 Signal on Dual-Located WHIRLY1 Associates with Leaf Senescence in Arabidopsis.
901 Cells 8:1585
902 Love AJ, Milner JJ, Sadanandom A (2008) Timing is everything: Regulatory overlap in
903 plant cell death. Trends Plant Sci 13(11):589–595;
904 Lv R, Li Z, Li M, Dogra V, Lv S, Liu R, Lee KP, Kim C. (2019) Uncoupled Expression of
905 Nuclear and Plastid Photosynthesis-Associated Genes Contributes to Cell Death in
906 a Lesion Mimic Mutant. Plant Cell 31(1):210-230.
907 Martínez C, Pons E, Prats G, León J. (2004) Salicylic acid regulates flowering time
908 and links defence responses and reproductive development. Plant J 37(2):209-17.
909 Melonek J, Mulisch M, Schmitz-Linneweber C, Grabowski E, Hensel G, Krupinska K
910 (2010) Whirly1 in chloroplasts associates with intron containing RNAs and rarely
911 co-localizes with nucleoids. Planta 232: 471-481
912 Miao Y, Jiang J, Ren Y, Zhao Z (2013) The single-stranded DNA-binding protein
913 WHIRLY1 represses WRKY53 expression and delays leaf senescence in a
914 developmental stage-dependent manner in Arabidopsis. Plant Physiol 163:
915 746-756
916 Miao Y, Zentgraf U (2007) The antagonist function of Arabidopsis WRKY53 and
917 ESR/ESP in leaf senescence is modulated by the jasmonic and salicylic acid
918 equilibrium. Plant Cell 19: 819-830
919 Morris K., Soheila A.-H.-M., Page T., John C. F., Murphy A. M., Carr J. P., et al. (2003).
920 Salicylic acid has a role in regulating gene expression during leaf senescence.

921 Plant J 23, 677–685.

922 Nevarez PA, Qiu Y, Inoue H, Yoo CY, Benfey PN, Schnell DJ, Chen M (2017)
923 Mechanism of Dual Targeting of the Phytochrome Signaling Component
924 HEMERA/pTAC12 to Plastids and the Nucleus. Plant Physiol 173: 1953-1966

925 Park SW, Kaimoyo E, Kumar D, Mosher S, Klessig DF (2007) Methyl salicylate is a
926 critical mobile signal for plant systemic acquired resistance. Science
927 318(5847):113–116.

928 Pesaresi P, Kim C (2019) Current understanding of GUN1: a key mediator involved in
929 biogenic retrograde signaling. Plant Cell Rep 38(7):819-823.

930 Prikryl J, Watkins KP, Friso G, van Wijk KJ, Barkan A (2008) A member of the Whirly
931 family is a multifunctional RNA- and DNA-binding protein that is essential for
932 chloroplast biogenesis. Nucleic Acids Res 36: 5152-5165

933 Rao MV, Paliyath G, Ormrod DP, Murr DP, Watkins CB (1997) Influence of salicylic
934 acid on H2O2 production, oxidative stress, and H2O2-metabolizing enzymes.
935 Salicylic acid-mediated oxidative damage requires H2O2. Plant Physiol 115:
936 137-149

937 Rekhter D, Lüdke D, Ding Y, Feussner K, Zienkiewicz K, Lipka V, Wiermer M, Zhang Y,
938 Feussner I (2019) Isochorismate-derived biosynthesis of the plant stress hormone
939 salicylic acid. Science 365, 498–502

940 Ren Y, Li Y, Jiang Y, Wu B, Miao Y (2017) Phosphorylation of WHIRLY1 by CIPK14
941 Shifts Its Localization and Dual Functions in Arabidopsis. Mol Plant 10: 749-763

942 Rivas-San Vicente M, Plasencia J (2011) Salicylic acid beyond defence: Its role in
943 plant growth and development. J Exp Bot 62(10):3321–3338.
944 Rohde A, Morreel K, Ralph J, Goeminne G, Hostyn V, De Rycke R, Kushnir S, Van
945 Doorsselaere J, Joseleau JP, Vuylsteke M, Van Driessche G, Van Beeumen J,
946 Messens E, Boerjan W (2004) Molecular phenotyping of the pal1 and pal2 mutants
947 of Arabidopsis thaliana reveals far-reaching consequences on phenylpropanoid,
948 amino acid, and carbohydrate metabolism. Plant Cell 16: 2749-2771
949 Sardar A, Nandi AK, Chattopadhyay (2017) CBL-interacting protein kinase 6
950 negatively regulates immune response to Pseudomonas syringae in Arabidopsis. J
951 EXp Bot 68(13):3573-3584
952 Sarrion-Perdigones A, Vazquez-Vilar M, Palací J, Castelijns B, Forment J, et al. (2013)
953 GoldenBraid 2.0: A Comprehensive DNA Assembly Framework for Plant Synthetic
954 Biology. Plant Physiol 162: 1618–1631
955 Sun X, Feng P, Xu X, Guo H, Ma J, Chi W, Lin R, Lu C, Zhang L (2011) A chloroplast
956 envelope-bound PHD transcription factor mediates chloroplast signals to the
957 nucleus. Nat Commun 2: 477
958 Swida-Barteczka A, Krieger-Liszkay A, Bilger W, Voigt U, Hensel G,
959 Szweykowska-Kulinska Z , Krupinska K (2018) The plastid-nucleus located
960 DNA/RNA binding protein WHIRLY1 regulates microRNA-levels during stress in
961 barley (*Hordeum vulgare* L.). RNA Biol DOI: 10.1080/15476286.2018.1481695
962 Thimm O, Blasing O, Gibon Y, Nagel A, Meyer S, Kruger P, Selbig J, Muller LA, Rhee

963 SY, Stitt M (2004) MAPMAN: a user-driven tool to display genomics data sets onto
964 diagrams of metabolic pathways and other biological processes. Plant J 37:
965 914-939
966 Torrens-Spence M, Bobokalonova A, Cartallo V, Glinkerman C, Pluskai T, Weng J
967 (2019) PBS3 and EPS1 complete salicylic acid biosynthesis from isochorismate in
968 Arabidopsis. Mol Plant DOI:j.molp.2019.11.005
969 Vallon O, Hoyer-Hansen G, Simpson DJ (1987) Photosystem II and cytochrome b559
970 in the stroma lamellae of barley chloroplasts. Carlsberg Research Communications
971 52: 405-421
972 Verberne MC, Brouwer N, Delbianco F, Linthorst HJ, Bol JF, Verpoorte R (2002)
973 Method for the extraction of the volatile compound salicylic acid from tobacco leaf
974 material. Phytochem Anal 13: 45-50
975 Vlot AC, Dempsey DA, Klessig DF (2009) Salicylic acid, a multifaceted hormone to
976 combat disease. Annu Rev Phytopathol 47:177–206.
977 Vogelmann K, Drechsel G, Bergler J, Subert C, Philippar K, Soll J, Engelmann JC,
978 Engelsdorf T, Voll LM, Hoth S (2012) Early senescence and cell death in
979 Arabidopsis saul1 mutants involves the PAD4-dependent salicylic acid pathway.
980 Plant Physiol 159: 1477-1487
981 Wang X, Ding Y, Li Z, Shi Y, Wang J, Hua J, Gong Z, Zhou JM, Yang S (2019) PUB25
982 and PUB26 Promote Plant Freezing Tolerance by Degrading the Cold Signaling
983 Negative Regulator MYB15. Dev Cell 51(2):222-235

984 Wildermuth MC, Dewdney J, Wu G, Ausubel FM (2001) Isochorismate synthase is
985 required to synthesize salicylic acid for plant defence. Nature 414(6863):562–565.
986 Woodson JD, Perez-Ruiz JM, Chory J (2011) Heme synthesis by plastid
987 ferrochelatase I regulates nuclear gene expression in plants. Curr Biol 21: 897-903
988 Woodson JD, Perez-Ruiz JM, Schmitz RJ, Ecker JR, Chory J. (2013) Sigma
989 factor-mediated plastid retrograde signals control nuclear gene expression. Plant J
990 73(1):1-13.
991 Wu GZ, Meyer EH, Richter AS, Schuster M, Ling Q, Schöttler MA, Walther D, Zoschke
992 R, Grimm B, Jarvis RP, Bock R. (2019) Control of retrograde signalling by protein
993 import and cytosolic folding stress. Nat Plants 5(5):525-538.
994 Xiong JY, Lai CX, Qu Z, Yang XY, Qin XH, Liu GQ (2009) Recruitment of AtWHY1 and
995 AtWHY3 by a distal element upstream of the kinesin gene AtKP1 to mediate
996 transcriptional repression. Plant Mol Biol 71: 437-449
997 Yamamoto S, Katagiri M, Maeno H, Hayaishi O (1965) Salicylate hydroxylase, a
998 monooxygenase requiring flavin adenine dinucleotide: I. purification and general
999 properties. J Biol Chem 240(8):3408–3413.
1000 Yoo HH, Kwon C, Lee MM, Chung IK (2007) Single-stranded DNA binding factor
1001 AtWHY1 modulates telomere length homeostasis in Arabidopsis. Plant J 49:
1002 442-451
1003 Zhang K, Halitschke R, Yin C, Liu C, and Gan S (2013) Salicylic acid 3-hydroxylase
1004 regulates Arabidopsis leaf longevity by mediating salicylic acid catabolism. PNAS

110 (36): 14807–14812

Zhang Z, Li Q, Li Z, Staswick PE, Wang M, Zhu Y, He Z (2007) Dual regulation role of GH3.5 in salicylic acid and auxin signaling during Arabidopsis-Pseudomonas syringae interaction. Plant Physiol 145(2):450–

Zhao Y, Luo L, Xu J, Xin P, Guo H, Wu J, Bai L, Wang G, Chu J, Zuo J, Yu H, Huang X and Li J (2018) Malate transported from chloroplast to mitochondrion triggers production of ROS and PCD in Arabidopsis thaliana. Cell Research 28:1-14

Figure legends

Figure 1. The variation transcript level of genes encoding key enzymes related to SA metabolism pathway and SA contents in the *why1* line during the development

a. SA metabolism pathway in the cell. b The variation transcript level of genes encoding key enzymes related to SA metabolism in the *why1* line during plant development. c. Content of conjugated (C-SA) and free (F-SA) salicylic acid in wild type and *why1* mutant during the period of 28 to 55 days after germination (dag); d. Changes of conjugated and free salicylic acid contents in a series of double mutants with focus on 37 and 42 dag. f. Senescence phenotype of 37 dag old double mutants.

The relative expression level normalized to GAPC, wild type at 28 dag (b) was setup as 1. The standard error bars present three time biological replicates and three time techniques replicates, the values are shown as means ±SD. Asterisks (*P < 0.05, **P < 0.01) show significant differences to wild type line according to either two-way ANOVA or pair-wide

multiple t-tests.

Figure 2. Transcript level analysis of genes encoding key enzymes related to SA metabolism pathway (a) and SA contents (b) in the pWHY1/why1, nWHY1/why1, and pnWHY1/why1 transgenic plants compared to wild type from 28 to 42 dag during plant development. The standard error bars present three time biological replicates, the values are shown as means±SE. Asterisks (*P < 0.05, **P < 0.01) show significant differences to WT within the respective conditions according to Student's t test.

Figure 3. The VEX:pWHY1, VEX:nWHY1 and the why1 mutants exhibits a complex nuclear genetic reprogramming.

a. MapMan analysis for gene ontology terms enrichment of the entire *VEX:pWHY1*, *VEX:nWHY1* and the *why1* nuclear transcriptome.

b. Histogram presenting the ratio of differentially expressed genes enrichment changes of selected biological process of the *VEX:pWHY1, VEX:nWHY1* and the *why1* transcriptome.

c. The heatmap of SA metabolism related gene expression levels of the *pWHY1/why1*, *nWHY1/why1*, *pnWHY1/why1* plants, and the *why1* mutants. *VEX:pWHY1*, *VEX:pWHY1/why1; VEX:nWHY1, VEX:nWHY1/why1*

Figure 4. WHY1 activates/represses target gene expression

b. Enrichment profiles of WHY1 protein in five target genes: *ERF109, MYB15, ICS1*, *WRKY53,* and *WRKY33* by ChIP-seq; b.Position of promoter motives (*GTNNNNAAT plus AT-rich*) of WHY1 target genes; c. Enrichment folds of WHY1 at the promoters of target genes by ChIP-qPCR at 37 and 42 days after germination; d. The expression levels of target genes

1047 at 37 and 42 days after germination in the *why1* mutant compared to WT. The error bars
1048 represented SD from three biological replicates. Asterisks indicated significant differences
1049 from the ACTIN according to two-tail Student's t test (* denotes P < 0.05, ** for P < 0.01).
1050 Figure 5. Promoter activation assays using the LUC/REN system
1051 a. Structure of activator and reporter constructs. b. The promoters of *ICS1, MYB15, ERF109,*
1052 *WRKY53*, and *WRKY33* genes are co-infiltrated with a vector containing WHY1 under the
1053 regulation of the ACTIN promoter. c, Co-infiltration of MYB15 and ERF109 with the *PAL1,*
1054 *PAL2, ICS1,* and *BSMT1* promoters. Background promoter activity is assayed by
1055 co-infiltration with an empty vector of the same type. Shown are means and SE of six
1056 biological replicates. Asterisks denote statistically significant differences from the empty
1057 vector calculated using Student's t test: *, P , 0.05; **, P , 0.01; and ***, P , 0.001.
1058 Figure 6. Phenotyping of loss- of *WHY1* and its downstream target genes mutants
1059 a. Phenotypes of loss-of *PAL1, ICS1, MYB15* and *BSMT1* at 37dag compared to *WHY1*
1060 mutants. Whole rosette (a-up) and senescent leaf ratio of 5 plants (a-down); b. ROS
1061 accumulation of loss-of *PAL1, ICS1, MYB15* and *BSMT1* at 37dag compared to *WHY1*
1062 mutants by NBT and DAB staining; c. The transcript levels of SAGs genes in the loss- or gain-
1063 of *PAL1, BSMT1* and loss- of *MBY15, ERF109* and *ICS1* plants at 37dag by qRT-PCR. The
1064 standard error is calculated from three biological replicates, the values are shown as
1065 means±SE, the wild-type was setup to 1 in the heatmap.
1066 Figure 7. The plastid and nuclear isoform WHY1 protein immunodetection after the treatment
1067 of MeSA and in the *sid2, pal1* or double *sid2 pal1* mutants compared to WT

a. The expression level of WHY1 in the WT plants after MeSA treatment for 1, 2, 4, 6, 8 hrs; b. WHY1 immunodetection in nuclear extracts after the treatment of MeSA for 4 hours, and in the *sid2, pal1* or double *sid2 pal1* mutants compared to WT; c. WHY1 immunodetection in plastid extracts after the treatment of MeSA for 4 hours, and in the *sid2, pal1* or double *sid2 pal1* mutants compared to WT. Coomassie and silver staining as the protein amount loading controls. L-WHY1: large size (37 kDa) of WHY1; S-WHY1: small size (29 kDa) of WHY1. The antibody against peptide WHY1 was prepared by company; d. The alteration of pWHY1 and nWHY1 after MeSA treatment or in the sid2, pal1 or double sid2 pal1 mutants compared to WT. The protein band signal is captured and calculated by Image J software program (http://www.di.uq.edu.au/ sparqimagejblots). The data shows the average of three replicates. Asterisks (*P < 0.05, **P < 0.01) show significant differences to H_2O treatment or WT according to Student's t test.

Figure 8. A working model of the senescence pathway performed by the dual located WHY1 in response to SA. The nuclear isoforms of WHY1 are represented as both a large molecular mass (37 kDA, bigger letters in the Figure) and a small molecular mass (29 kDa, smaller letters). WHY1 has dual functions in plastids and the nucleus. Loss of WHY1 increases SA accumulation at early stage (37 dag) through increasing PAL1 expression and repressing BSMT1; Elevated SA promotes nuclear WHY1 de-modification and promotes ICS1 and BSMT1 expression thereby balancing SA homeostasis in the cells. High SA levels by ICS1 cause feedback enhancing ROS accumulation, promoting senescence. pWHY1 stimulates PAL1/ICS1 expression but represses BSMT1, allowing high levels of SA, leading also to early

1089 senescence. Thus, distribution of WHY1 organelle isoforms and the putative feedback of SA
1090 form a circularly integrated regulatory network during plant senescence in a developmental
1091 dependent manner. Plastid (Chl) is shown as a green ovary, nucleus (Nuc) as a grey ovary,
1092 lines for regulation, fat arrows for transfer or translocation, broken lines for uncertainty